REVIEW OF METHANE SLIP FROM LNG ENGINES

NIINA KUITTINEN
MIKKO HEIKKILÄ
KATI LEHTORANTA

GREEN RAY

The GREEN RAY project has received funding from the European Union's Horizon Europe research and innovation programme under grant agreement N°101056642.

DELIVERABLE DESCRIPTION

Grant Agreement Number	101056642
Project Acronym	GREEN RAY
Project Title	New GeneRation marinE ENgines and Retrofit solutions to Achieve methane abatement flexibilitY
Project Call	HORIZON-CL5-2021-D5-01-12
Project Duration	60 months: 1 June 2022 – 31 May 2027
Deliverable Number	D1.1
Deliverable Title	Review of methane slip from LNG marine engines
Deliverable Type	Report
Security Classification	Public
Contributing Work Package	WP1
Lead Partner	VTT Technical Research Centre of Finland
Contributing Partners	Finnish Meteorological Institute, Shell Global Solutions, Wartsila Finland, Wartsila Italia, MSC, CMA Ships, Chantiers de l'Atlantique
Version	v2
Authors	Niina Kuittinen, Mikko Heikkilä, Kati Lehtoranta
Reviewer	Jukka-Pekka Jalkanen
Contractual Delivery Date	31.1.2023

GREEN RAY

Keywords list
LNG engines, methane slip, methane emission factors, review

GREEN RAY Consortium

VTT (Teknologian Tutkimuskeskus VTT Oy)

FMI (Finnish Meteorological Institute)

Shell (Shell Global Solutions International BV)

CdA (Chantiers de l'Atlantique)

WIT (Wärtsilä Italia Spa)

WFI (Wärtsilä Finland Oy)

DNV (DNV AS)

MSCMYM (MSC Malta Yard Management Ltd)

CMA (CMA Ships)

WSCH (Wärtsilä Services Switzerland AG)

MSC (MSC Cruise Management UK Limited)

REV (Revolve Water)

Table of Contents

LIST OF ABBREVIATIONS

AIS	Automatic Identification System
BC	Black carbon
BSEC	Break Specific Energy Consumption
CEMS	Continuous emission monitoring system
CF	Carbon Factor
CH_4	Methane
CO	Carbon monoxide
CO_2	Carbon dioxide
DCS	IMO Data Collection System for fuel oil consumption on ships
DF	Dual-fuel engine technology
ETS	Emissions Trading System
EU	European Union
EC	Elemental carbon
FSRU	Floating Storage Regasification Unit
FSU	Floating Storage Unit
GHG	Greenhouse Gas
GWP	Global Warming Potential
HCHO	Formaldehyde
HPDF	High Pressure Dual Fuel
IGF Code	International Code of Safety for Ships Using Gases or Other Low-flashpoint Fuels
IMO	International Maritime Organization
LBSI	Lean Burn Spark Ignited engine
LNG	Liquefied Natural Gas
LPDF	Low Pressure Dual Fuel engine
MARPOL	International Convention for the Prevention of Pollution from Ships
MRV	EU Monitoring, Reporting, and Verifying open-access database
NMHC	Non-methane hydrocarbons
N_2O	Nitrous oxide
NO_x	Nitrogen oxides (NO, NO_2)
OC	Organic carbon
PM	Particle mass
PN	Particle number
STEAM	Ship Traffic Emission Assessment Model developed by Finnish Meteorological Institute
THC	Total hydrocarbons
TtW	Tank-to-wake
ULSD	Ultra-low sulfur diesel
WtT	Well-to-tank
WtW	Well-to-wake

1. Introduction

The use of liquefied natural gas (LNG) as shipping fuel has increased in recent years and it has direct effects, namely benefits, on air quality and human health. According to a recent report, about 20% of the total vessel orders in 2021 were LNG-fueled (Plevrakis et al., 2022). Vessels using LNG as fuel enable one transition pathway from fossil to non-fossil fuels. In such a transition, methane molecules, which are the main component of LNG, can be considered as a drop-in fuel, compatible with existing marine engines. Methane may be of fossil, bio, or synthetic origin, but it needs to be produced in large enough quantities. Further, the origin of the biomaterial and electricity used in fuel synthesis must be sustainable. LNG can be considered as a transition fuel which facilitates the decarbonization of maritime transport. Ideally, existing engine solutions and tank arrangements can be used with very low or zero carbon fuels with minimal need of modifications (Lindstad et al., 2020; Plevrakis et al., 2022). The utilization of LNG in dual-fuel (DF) engines together with liquid fuel for ignition also allows fuel flexibility for the ship operators.

LNG is mainly composed of methane (CH_4) which has higher hydrogen-carbon ratio and energy content compared to liquid fuels, leading to lower emissions of carbon dioxide (CO_2). The use of LNG as marine fuel can also reduce the emissions of nitrogen oxides and particulate matter including black carbon, relative to operation on marine gas oil (Aakko-Saksa et al., 2023; Anderson et al., 2015; Lehtoranta et al., 2019; Peng et al., 2020). In comparison to heavy fuel oil, natural gas combustion has been estimated to produce a unit of energy with 24% less carbon dioxide emissions, 90-99% less sulfuric oxides, and 90% less particulate matter (Mærsk Mc-Kinney Møller Center for Zero Carbon Shipping, 2022). While the use of LNG has benefits in terms of CO_2 emissions and local air pollutants, emission of unburnt methane to atmosphere remains a concern.

In the atmosphere, methane is an important greenhouse gas (GHG) contributing to climate change. On instantaneous basis, methane is 120 times stronger absorber of infrared radiation than CO_2, but its atmospheric lifetime of 12 years is shorter compared to CO_2 which can remain in the atmosphere hundreds of years. Considering a 100-year timescale, methane has 28-30 times greater global warming potential (GWP) than carbon dioxide and is 84 times more potent on a 20-year timescale (Myhre et al., 2013). Thus, methane emissions are considered highly relevant to 2050 climate objectives (European Commission, 2022). In addition to being a greenhouse gas, methane contributes to ozone formation which is a local air pollutant. Due to the high GWP of methane, even low emissions may negate the CO_2 benefits of switching to LNG from heavy fuel oil or marine diesel oil. (Balcombe et al., 2022).

Methane emissions occurring from the carriage and consumption of LNG as fuel in marine vessels can occur as fugitive emissions, through venting, or via methane slip from the engines. In a recent study on-board an LNG carrier during a transatlantic voyage, it was found that methane slip from main and auxiliary engines accounted 99% of methane emissions across the voyage and 35% of total GHG emissions of the voyage on this specific ship (Tank-to-Wake, TtW), representing a significant opportunity for mitigation through the study and development of engine technology. In a study considering the total Well-to-Wake (WtW) GHG emissions of LNG fueled engines by applying extensive life cycle analysis approach and data from several engine manufacturers, unburned methane has been reported to contribute up to 22%, methane slip during combustion (TtW) accounting for 16%, and methane emissions in the supply chain (Well-to-Tank, WtT) 6% of the total GHG emissions (Schuller et al., 2021). A need for reducing TtW methane slip emissions has also been recognized in order to increase viability of electro- and biomethane fuel pathways (Mærsk Mc-Kinney Møller Center for Zero Carbon Shipping, 2022).

Globally, LNG use as maritime fuel is regulated with the International Convention for the Prevention of Pollution from Ships (MARPOL) and the International Code of Safety for Ships Using Gases or Other Low-flashpoint Fuels (IGF Code), which defines the needed technical requirements and procedures for carriage and combustion of natural gas as maritime fuel. Regulations neither limit methane emissions as product of combustion, nor are methane emissions counted in any regulations set by the International Maritime Organization (IMO) concerning GHG emissions or energy efficiency. However, the IGF Code stipulates that venting fuel vapor from LNG tanks is not allowed except in an emergency. The transformation of parts of liquefied fuel into gaseous form (to so called boil-off) by the ambient temperature should be controlled by either reliquefying, combustion, pressure accumulation, or by cooling of the liquefied gas fuel (IMO, 2022b).

Currently, the European Union (EU) is in the process of issuing amendments for directives that regulate maritime transport as part of the Green Deal and Fitfor55 environmental packages. Two specific regulations will affect methane emissions from ships: the Emissions Trading System (ETS) and the FuelEU Maritime. Both have passed the EU Parliament vote and are currently being negotiated between the European Commission, Parliament, and member states. Both mechanisms will include carbon dioxide, methane, and nitrous oxide (N_2O) GHG emissions from the maritime transport (European Parliament, 2022b, 2022a). ETS will consider emissions on Tank-to-Wake basis and the FuelEU Maritime on Well-to-Wake basis. In the FuelEU Maritime, the effect of methane slip is introduced as a percentage of the mass of the fuel used by the engine (Mærsk Mc-Kinney Møller Center for Zero Carbon Shipping, 2022). Additionally, global attempt to mitigate methane emissions was agreed on in COP26 United Nations Climate Change Conference where the United States, the EU and 100 other countries signed their Global Methane Pledge, aiming to cut methane emissions by 30% by 2030 compared to 2020 levels (Global Methane Pledge, 2021).

This report focuses on collecting information on the methane emissions that originate when unburned methane exits the ship engines. Methane slip reduction has been recognized as a topic for engine manufacturers for over 10 years and mitigation of methane slip is enabled both by developing engine technology, after-treatment technologies as well as vessel specific systemic solutions (Mærsk Mc-Kinney Møller Center for Zero Carbon Shipping, 2022). However, numerical data of methane slip from marine engines in the literature is scarce, especially for the engines build in the recent years, posing a challenge for the estimation of total methane slip emissions from shipping today and constructing scenarios for the future. The aim of this work is to provide an overview of the published methane slip emission factors as well as to complement the existing values by collecting ship owner data covering measurements conducted on newly build engines (years 2019-2022).

2. Methodology

The modular Ship Traffic Emission Assessment Model (STEAM) (e.g. Johansson et al., 2017) developed at the Finnish Meteorological Institute (FMI) was used to identify the number of LNG powered vessels currently in operation and the shares of different LNG engine types installed. STEAM combines global Automatic Identification System (AIS) data (obtained from Orbcomm Ltd.) with a database that is updated using the IHS Markit ship information service. Among other data, the database contains information on each vessel's main and auxiliary engine fuel type and engine model. The engine model is connected with an engine database which contains data of known LNG engine models. Currently, the LNG engine model database contains 323 engine models with their respective model code, engine manufacturer, Break Specific Energy Consumption (BSEC) at 80% engine load, engine speed in rpm, LNG engine type, and the engine load below which engine operates only on liquid fuel. STEAM modelling results and AIS data from 2021 were used for this review.

Information of LNG use as maritime fuel was collected from the International Maritime Organization Data Collection System for fuel oil consumption on ships (DCS), which has been storing reports since 1st of January 2019 (IMO, 2022a). At the time of the study, reports for years 2019, 2020, and 2021 were available. As per the reports, 27 221 vessels out of the 32 511 vessels under the scope (84%) reported their fuel consumption to DCS in 2019, 27 723 vessels out of 32 558 in 2020 (85.1%) and 28 171 out of 32 998 (85.4%) in 2021. Therefore, the absolute reported fuel masses do not represent 100% of fuel combusted at sea, but the share of LNG use by different vessel types should be representative. LNG-powered vessels sailing in Europe were investigated using the EU Monitoring, Reporting and Verifying (MRV) open-access database (mrv.emsa.europe.eu). Reports from 2018-2021 were available, and the EMSA dataset versions used were 267 for 2018, 208 for 2019, 166 for 2020, and 90 for 2021.

Information of methane slip as well as other exhaust emissions from LNG engines was collected both from published literature as well as by including ship owner data for engines from recent years. Emission factors for methane were collected in brake specific terms (g/kWh) when available, or as percentage of fuel burned. List of all engines for which methane emission data was identified are listed in Appendix A. The engine construction years for which methane slip results have been reported in the literature are 2010 (and older / newer), 2012, 2013 (and newer), 2016, 2016 (retrofitted), and 2021. One of the main aims of this report is to complement the reported methane slip data with values from engines designed and built in the recent years (2019-2022) to provide an understanding of the current methane slip status from modern LNG engines. The engine construction year is taken directly when reported, and in other cases the building year of the vessel is assumed. If neither engine construction year nor building year of the vessel is reported, publication year is indicated (marked as publ.). It should be noted that the engine construction year does not always indicate the technology level, because old engine technology can be installed on new ships. However, in this report it is not possible to distinguish the year of the engine design as it is typically not mentioned in public reports or articles, therefore engine (or vessel) building year is used.

In this report, the LNG engines available in the marine market are divided in four categories according to the engine type:

- *Type 1: Lean Burn Spark Ignited engines (LBSI)*
- *Type 2: 4-stroke Low Pressure Dual Fuel engines (LPDF 4-S)*
- *Type 3: 2-stroke Low Pressure Dual Fuel engines (LPDF 2-S)*
- *Type 4: 2-stroke High Pressure Dual Fuel engines (HPDF 2-S)*

Type 1 engines include Lean Burn Spark Ignited (LBSI) engines utilizing only natural gas as fuel with spark plug ignition. The LBSI engines are typically 4-stroke high or medium speed engines utilized in smaller vessel types and where fast engine response is needed (Schuller et al., 2021). Type 2 category includes 4-stroke Low Pressure Dual Fuel (LPDF 4-S) engines where natural gas is injected in low pressure during the compression stroke of the engine and small amount of liquid fuel is used for ignition. The LPDF 4-S engines typically operate with medium speed and typically allow more flexible operation than their 2-stroke counterparts. They are mostly utilized in ferries, cruise ships, and short sea shipping as well as auxiliary engines at large vessels. (Schuller et al., 2021). Low Pressure Dual Fuel engines operating with 2-stroke cycle (LPDF 2-S) are categorized as Type 3. The LPDF engines operate according to the thermodynamic Diesel cycle in liquid fuel mode and according to Otto cycle in LNG mode, therefore in some sources they are also referred to as Otto-DF engines. Finally, Type 4 engines include 2-stroke High Pressure Dual Fuel engines where natural gas is injected in high pressure at the end of compression stroke, simultaneously with the liquid pilot fuel injection. These engines are categorized as slow speed and operate according to Diesel cycle also during LNG operation, therefore referred to also as Diesel-DF engines. The 2-stroke engine types have the highest efficiency and power and are commonly used in large ocean-going cargo ships (Schuller et al., 2021).

LPDF 4-S engines were found to be most widely covered in the scientific literature with at least one publication including results for LPDF 2-S engines. As seen in section 3.3, LPDF 4-S and LPDF 2-S engines are most widely used engines and therefore these engine types were also in the main focus of the review. LBSI engines are mainly used in smaller vessel categories, but their methane slip was included when reported in the publications. Original measurement data for HPDF engines were found to be lacking from the scientific literature but few values given by engine manufacturer were included in reports. Generally, the methane slip from HPDF engines is considered low due to the applied injection and combustion method.

The choice of engines for a vessel is dependent at least on the ship type, size, and operational parameters. Large container ships often use 2-stroke engines and mainly operate in deep-sea regions where they may apply constant engine load for long periods after exiting the harbor. On the other hand, ferries or cruise ships are typically equipped with 4-stroke engine and operate on coastal areas where engine load changes may be more frequent. For small ships and tugboats, engine response with many load changes is needed. (Schuller et al., 2021). To consider these varying operational patterns with different engine types, the methane slip values are presented as function of engine load percentage when the load-dependent data is available. In some cases, emission factors found in the literature were presented as weighted emissions according to the established ISO 8178 E3/E2 test cycles, where different fixed load conditions of 100%, 75%, 50%, and 25% are weighted with factors of 0.2, 0.5, 0.15, and 0.15. Thus, in the results reported according to the standardized cycle, engine operation at high load conditions in emphasized (Dieselnet, 2022).

3. LNG ships and engines

3.1. LNG as marine fuel

Natural gas consists primarily of methane, but its composition varies according to region with varying share of alkanes such as ethane, propane, and isobutane. For transport overseas and use as marine fuel, natural gas is liquefied in a process that cools the pre-treated gas down to a liquid form in -162°C. Liquefaction allows storing natural gas in 600 times lower volume than gas in standard atmospheric pressure. (European Commission, 2023; Pavlenko et al., 2020). Globally, the United States, Australia, and Qatar were the largest LNG exporters in 2022, whereas largest exporters to the EU in the first half of 2022 were the United States, Russia, and Qatar with agreement to increase trade from the United States (European Commission, 2023). Ushakov et al. (2019) collected the composition of LNG from several suppliers in Europe (Table 1), where the methane content varied between 91-96%, ethane content between 3-7%, and propane content between 0.3-1.4%. Methane content in LNG sources from different continents (according to Kuczynski et al., 2020) can vary from 87.3 to up to 99.7%, ethane between 0.09-9.97%, and propane between 0.03-3.3%.

Table 1. LNG composition from different suppliers across Europe and from various export sources (synthesized from Kuczynski et al., 2020; Ushakov et al., 2019*).*

Component	Unit	Gasnor, Kollsnes (NO)		Titan LNG, Moerdijk (NL)	Statoil, Hammerfest (NO)	Bahia de Bizkaia Gas, Bilbao (ES)	Skangas, Risavika (NO)
Methane	mol-%	95.901	94.593	91.185	92.106	91.908	92.270
Ethane	mol-%	3.037	3.828	6.923	5.591	7.039	6.873
Propane	mol-%	0.370	0.575	1.407	1.233	0.674	0.417
Isobutane	mol-%	0.142	0.286	0.140	0.118	0.083	0.030
n-Butane	mol-%	0.001	0.070	0.288	0.297	0.098	0.040
Isopentane	mol-%	0.019	0.073	0.016	0.014	0.005	0.003
n-Pentane	mol-%	0	0	0.004	0.003	0.001	0
Nitrogen	mol-%	0.530	0.592	0.036	0.638	0.929	0.370
Gross Calorific Value	MJ/kg	54.737	54.560	54.993	n/a	n/a	54.740
Net Calorific Value	MJ/kg	49.383	49.338	49.578	49.169	49.554	49.380
Density	kg/m^3	0.747	0.756	0.789	0.781	0.775	0.772
Methane number		85.5	81.0	76.4	78.6	79.8	81.6
		Australia, NWS	Australia, Darwin	Norway	Qatar	Russia, Sakhalin	USA, Alaska
Methane	%	87.33	87.64	92.03	90.91	92.54	99.7
Ethane	%	8.33	9.97	5.75	6.43	4.47	0.09
Propane	%	3.33	1.96	1.31	1.66	1.97	0.03
C4+	%	0.97	0.33	0.45	0.73	0.95	0.01
Nitrogen	%	0.04	0.1	0.46	0.27	0.07	0.17

According to the IMO DCS data, the total reported use of LNG as maritime fuel was 10 482 742 metric tons in 2019, 11 974 761 metric tons in 2020 and 12 623 121 metric tons in 2021 (IMO, 2022a). Out of all combusted maritime fuel, this represents a share of 4.9% in 2019 (total 213 026 342 metric tons), 5.9% in 2020 (total 203 103 633 metric tons) and 5.9% in 2021 (total 212 230 077 metric tons). These numbers cover the ships with an IMO registry number over 5000 gross tons who went through the DCS reporting (83.7% in 2019, 85.1% in 2020, and 85.4% in 2021). Most of the total LNG combusted was used by LNG carriers (71.5% in 2019, 77.5% in 2020 and 78.9% in 2021) then followed by gas carriers (26.1% in 2019, 19.2% in 2020 and 16.9%), which are vessels capable of carrying gaseous cargo such as propane. The remaining vessel types represented 2.4% of all LNG combusted in 2019, 3.3% in 2020, and 4.2% in 2021. LNG use by vessel type is presented in Table 2. LNG use increased by 14.2% in 2020 compared to 2019 and by 5.4% in 2021 compared to 2020.

Table 2. LNG use as maritime fuel and the share of total LNG use by vessel type as reported to IMO in 2019-2021.

	2019		2020		2021	
Vessel type	LNG use (t)	Share of total (%)	LNG use (t)	Share of total (%)	LNG use (t)	Share of total (%)
Bulk carrier	0	0.0	10 929	0.1	36 773	0.3
Combination carrier	0	0.0	0	0.0	0	0.0
Container ship	24 893	0.2	49 887	0.4	163 707	1.3
Cruise ship	23 209	0.2	20 109	0.2	59 796	0.5
Gas carrier	2 733 961	26.1	2 298 402	19.1	2 137 002	16.9
General cargo ship	8 025	0.1	7 498	0.1	4 052	0.0
LNG carrier	7 494 993	71.5	9 282 739	77.3	9 958 661	78.9
Others	43 399	0.4	37 162	0.3	40 203	0.3
Passenger ship	0	0.0	37 162	0.3	3 551	0.0
Refrigerated cargo carrier	0	0.0	0	0.0	0	0.0
Ro-Ro cargo ship	6 167	0.1	5 153	0.0	6 166	0.0
Ro-Ro cargo ship (vehicle carrier)	0	0.0	10 540	0.1	16 895	0.1
Ro-Ro passenger ship	69 381	0.7	129 613	1.1	94 802	0.8
Tanker	78 714	0.8	122 729	1.0	101 513	0.8
All vessel types	**10 482 742**		**12 011 923**		**12 623 121**	

LNG powered vessels sailing in Europe that reported to the MRV database were identified by having a carbon factor (CF) of less than 3.0 (Table 3). The CF was calculated by dividing the reported total annual CO_2 emissions with the reported total annual fuel consumed. Liquefied fuel oils have a CF > 3.0 and the CF of LNG is 2.7.

Table 3. Ships that reported to the MRV database in 2018-2021 and that had a carbon factor less than 3.0 by vessel type.

	2018		2019		2020		2021	
Vessel type	All	CF < 3.0	All	CF < 3.0	All	CF < 3.0	All	CF < 3.0
Bulk carrier	3 845	0	3 656	1	3 459	0	3 714	3
Chemical tanker	1 364	7	1 362	15	1 351	15	1 386	11
Container vessel	1 813	1	1 851	4	1 855	17	1 825	28
Container / Ro-ro	80	0	76	0	70	0	64	0
Gas carrier	321	25	342	25	343	25	327	14
General cargo ship	1 176	0	1 243	4	1 238	3	1 236	2
LNG carrier	213	172	257	210	267	220	287	247
Oil tanker	1 907	2	2 008	2	1 931	11	1 847	16
Other vessel types	126	2	142	3	138	5	149	2
Passenger ship	159	1	179	2	111	2	107	5
Refrigerated cargo carrier	145	0	145	0	145	0	153	0
Ro-pax ship	376	5	404	15	398	18	369	16
Ro-ro ship	272	0	277	0	243	0	224	0
Vehicle carrier	448	0	434	1	455	3	464	3
All ships	**12 245**	**215**	**12 376**	**282**	**12 004**	**319**	**12 152**	**347**

3.2. LNG vessel types

The FMI STEAM model and its databases were used to identify the number of LNG powered vessels currently in operation and the shares of different LNG engine types installed. The FMI ship database currently contains data of 113 133 vessels. Out of these, 614 vessels are equipped with a known LNG powered dual-fuel engine and 35 vessels were marked as using LNG for propulsion with an unknown engine model. By vessel type (Figure 1), the largest share of known dual fuel engines were installed on LNG tankers (339 vessels or 55.2% of all LNG-powered dual-fuel engine ships) followed by production tankers (45 or 7.3%), container vessels (34 or 5.5%), ro-ro vessels (30 or 4.9%) and crude oil tankers (30 or 4.9%). LNG tankers are known to use their transported cargo as fuel for propulsion and auxiliary needs. There are 707 LNG tankers in the FMI ship database out of which 666 were transmitting AIS data in 2021. The remaining LNG tankers (368) that did not have a known dual-fuel engine mostly have a steam turbine as main engine, some have a gas turbine, and a few are equipped with a conventional oil engine. This is in line with the LNG-industry's own reporting. The International Gas Union annual report (International Gas Union, 2022) states that there were 641 active LNG tankers by the end of April 2022, including 45 Floating Storage Regasification Units (FSRU) and 5 Floating Storage Units (FSU). An interpretation of the IGU and other reports by American Bureau of Shipping gives a total of 694 LNG fueled ships either in operation or under construction as well as 213 more estimated to be LNG-ready (Plevrakis et al., 2022).

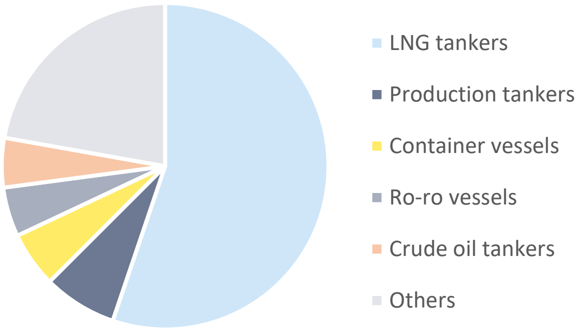

Figure 1. Share of known dual fuel engines in different vessel types.

Wartsila LPDF 4-S engines hold the largest share of installed dual-fuel engines (287 vessels or 46.7% of all LNG powered dual-fuel engine ships). WinGD LPDF 2-S engines were installed on 157 (25.6%) vessels. MAN engines were installed on 113 (18.4%) vessels out of which 17 had an LPDF 4-S and 96 an HPDF 2-S engine. The remaining manufacturer shares of dual fuel engines installed on vessels were: ABC (20 or 5.7% of all LPDF 4-S engines), Caterpillar (10 or 2.9%), Mitsubishi (6 or 1.7%), Niigata (4 or 1.1%), Hyundai (3 or 0.9%), MTU (2 or 0.6%) and Yanmar (1 or 0.3%). All installed Type 1 (LBSI) engines were manufactured by Bergen, all Type 3 (LPDF 2-S) were WinGD, and all Type 4 (HPDF) were MAN. 82% of all installed Type 2 (LPDF 4-S) engines were manufactured by Wartsila, 5.7% by ABC, 4.9% by MAN, 2.9% by Caterpillar, 1.7% by Mitsubishi, and 1.1% by Niigata.

3.3. LNG engines in operation

Out of the 614 vessels with an identified LNG engine, 11 were with Type 1 (LBSI) engine (1.7%), 350 with Type 2 (LPDF 4-S) engine (53.9%), 157 with Type 3 (LPDF 2-S) engine (24.2%) and 96 with Type 4 (HPDF) engine (14.8%). The distribution of engines by type is shown in Figure 2.

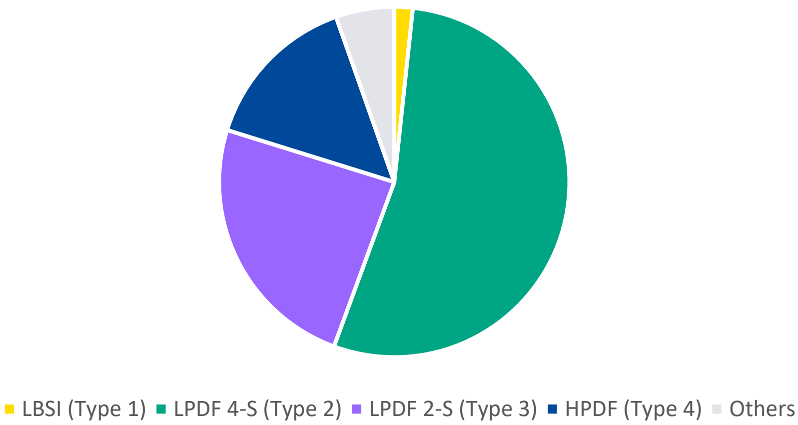

Figure 2. Distribution of engines by type in vessels identified with an LNG engine.

Out of the 614 dual fuel engine vessels in the FMI database, 508 were transmitting AIS data in 2021 and 588 vessels were modelled with STEAM as using LNG for propulsion. Maximum installed main engine power on the LNG-powered vessels were less than 5 000 kW (13.0% or 80 vessels), between 5 000 and 10 000 kW (14.3% or 88 vessels), between 10 000 and 25 000 kW (25.4% or 156 vessels), between 25 000 and 50 000 kW (41.2% or 253 vessels) and more than 50 000 kW (6.0% or 37 vessels), showing majority of ships with LNG engine to have maximum installed main engine power between 25-50 MW. Measured by the total installed main engine power (Figure 3), engine sizes below 5 MW represent 2% (installed power 298 MW), 5-10 MW engines 4% (629 MW), 10-25 MW engines 20% (3 026 MW), 25-50MW engines 59% (8 990 MW), and above 50 MW engines 15% of the total (15 246 MW).

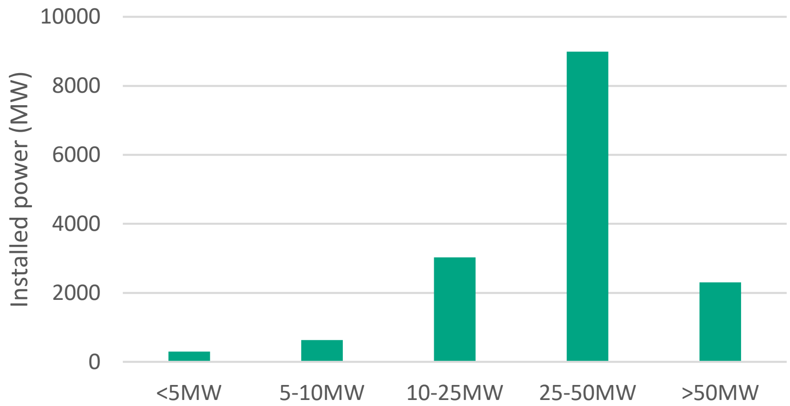

Figure 3. Distribution of total installed main engine power in LNG powered vessels by main engine power class.

3.4. Methane slip mechanisms

In LBSI engines (Type 1), the air-fuel mixture is ignited by spark plugs whereas in LPDF engines (Types 2&3) the ignition occurs as liquid diesel fuel (pilot fuel) is injected into the cylinder. In both engine types, the occurrence of methane slip can be explained either by temporary hiding of methane in cylinder crevices or quenching, both of which lead to a fraction of the injected natural gas to exit the engine unburned.

As natural gas is injected in low pressure during the early compression stroke and has time to reside in the cylinder before ignition, it may be pushed to the crevice volumes of the cylinder, including e.g., the gasket area between the cylinder head and cylinder liner, and remain unignited until slipping out of the cylinder during exhaust stroke. The mixing of the injected gas with air may also happen unevenly, creating gas-rich and gas-lean regions in the cylinder where also varying temperatures are reached.

Quenching can be explained as methane locally cooling down rapidly in the coldest areas of the combustion chamber, and as it requires a high temperature of >600°C to autoignite, remaining unburned. (e.g. Grönholm et al., 2021; Mærsk Mc-Kinney Møller Center for Zero Carbon Shipping, 2022). The lean combustion and consequent low thermal load may make the engine susceptible to quenching, especially at low engine loads when fuel-air ratio is lower (Heywood, 2019; Krivopolianskii et al., 2019; Stenersen, 2017, according to Lindstad et al., 2020). Sommer et al. (2019) showed an increase of methane emissions as a function of the air-fuel ratio, as operation at low loads results in leaner air-fuel mixtures and attributed the methane slip to decreased flame speeds in the leaner mixtures.

Methane slip may also be caused in LBSI and LPDF engines by direct slip due to valve overlap. If exhaust valve is partly open during gas admission, fraction of methane may flow directly to exhaust stack. In LPDF engines applying prechambers, incomplete combustion in prechamber is one additional potential source for methane slip (Winterthur Gas & Diesel Ltd, 2019).

GREEN RAY

More factors mentioned to affect methane slip are changes in natural gas composition and ambient conditions, as fuel composition and temperature both affect the optimal air-to-fuel ratio. During fluctuating load conditions (such as heavy weather) the turbocharger may also fail to follow changing air demand which may also alter the methane slip. Early or incomplete combustion leading to altered methane slip may also occur due to pre-ignition of lubrication oil or dripping fuel atomizers. (Mærsk Mc-Kinney Møller Center for Zero Carbon Shipping, 2022). In addition, evaporation from the lubricant oil film is stated as a known source of total hydrocarbon emissions which results from desorption of any formerly absorbed fuel molecules. (Winterthur Gas & Diesel Ltd, 2019)

In HPDF engines, natural gas is injected in high pressure together with the pilot fuel and combustion temperature is higher, therefore leading to lower susceptibility to quenching. Also, as the methane burns as it is being injected, there is less opportunities for methane residing in the crevice volumes. One potential phenomenon that could affect methane slip in HPDF engines is local flame extinction due to high turbulence. The low methane slip from HPDF engines can be seen as trade-off with NO_x emissions since the higher combustion temperature leads to NO_x levels requiring after-treatment to be IMO Tier III compliant. (Grönholm et al., 2021; Winterthur Gas & Diesel Ltd, 2019).

Recognized engine technologies for reducing methane slip include engine component design (e.g. minimizing crevices, piston ring design), high pressure injection (requiring gas compression equipment), engine tuning and control software (optimizing: valve timing, combustion timing, cylinder cut-off to enhance combustion velocity and decrease quenching, pilot fuel injection timing and quantity) as well as exhaust gas recirculation. The engine technologies can be applied either to new-build engines or as an upgrade to existing engines, but methane abatement has also been studied by utilizing after-treatment systems such as plasma reduction systems (application of high-voltage current to convert methane to CO and H_2O) or methane oxidation catalysts (requiring means to avoid sulfur poisoning of the catalyst). In the recent report by (Mærsk Mc-Kinney Møller Center for Zero Carbon Shipping (2022), 78% reduction was estimated for plasma reduction systems and 99% reduction was estimated possible for methane oxidation catalyst, however, targeting this high reduction could require very large catalyst surface, and thus 90% reduction could be a more realistic assumption. In addition, vessel specific system-based solutions, such as energy efficiency technologies, batteries, and shaft generators have been suggested to reduce total methane emissions. (Mærsk Mc-Kinney Møller Center for Zero Carbon Shipping, 2022).

4. Emissions from LNG engines

4.1. Reported data

The amount of methane slip data from LNG engines is limited and relies largely on measurement data from test-bed (Lehtoranta et al., 2019; Ushakov et al., 2019) or data provided by engine manufacturers (Lindstad et al., 2020; Mærsk Mc-Kinney Møller Center for Zero Carbon Shipping, 2022; Pavlenko et al., 2020; Rolls-Royce, 2012; Schuller et al., 2021; Stenersen & Thonstad, 2017) although a handful of studies (Anderson et al., 2015; Balcombe et al., 2022; Corbin et al., 2020; Peng et al., 2020; Sommer et al., 2019; Stenersen & Thonstad, 2017; Ushakov et al., 2019) which report original research data collected during on-board measurements are recognized. For the purposes of this study, ship owner data from 6 LPDF 2-S and 5 LPDF 4-S engines (listed in Appendix A) from years 2019-2022 were received to complement the data with methane slip information from recently build engines.

Majority of the found data considers methane slip from 4-stroke and 2-stroke LPDF engines, except few studies (Stenersen & Thonstad, 2017; Ushakov et al., 2019) which also included measurements of LBSI engines. The only data found for HPDF engines originates from engine manufacturers and no data including dependence of engine load or size was found. For these reasons and the targets of the GREEN RAY project, main attention on this report is given to LPDF engines. A list of all engines for which methane slip emission factors were found are given in Appendix A with their referenced sources.

In the publications which reported the applied measurement method for methane, (heated) flame ionization detection analyzer was most typically used (Anderson et al., 2015; Corbin et al., 2020; Peng et al., 2020; Sommer et al., 2019; Ushakov et al., 2019), in one case combined with gas chromatography (Anderson et al., 2015). Sommer et al. (2019) noted that since flame ionization detection is sensitive to all hydrocarbons, the efficiency of the catalytic cutter used to isolate other hydrocarbons from methane must be considered when reporting results. Fourier transform infrared spectroscopy has also been used in combination with gas chromatography (Lehtoranta et al., 2019) as well as stand-alone device in continuous emission monitoring system (CEMS) (Balcombe et al., 2022). Sommer et al. (2019) also introduced the use of custom-built methane sensor utilizing wavelength modulation spectroscopy. In cases where data originates from non-peer-reviewed literature such as from engine manufacture or ship owner, specific details of the measurement method are not available. It is recognized that more uniform guidelines for measuring methane concentration in the exhaust, converting it to emission factors as well as reporting could be beneficial.

If methane emissions are not measured directly, they may be reported as part of total or unburned hydrocarbons. Methane has been experienced to comprise 80 to 95% of unburned hydrocarbon emissions according to engine manufacturers, however this is highly dependent on the gas quality (Schuller et al., 2021). In the on-board study by Anderson et al. (2015) around 85% of the total hydrocarbons (THC) were found to be methane whereas Ushakov et al. (2019) reported 92-97% in their study. Lehtoranta et al. (2017) reported that at 85%/40% loads the THC in the exhaust contained 96.7%/96.5% of methane, 2.2%/2.3% ethane and 0.29%/0.13% propane, very close to the composition of the natural gas used in the study (96.4% methane, 2.3% ethane, 0.35% propane).

The methane slip from LNG engines can be described in various units. Firstly, ratio of fuel loss compared to total fuel consumed by the engine can be expressed as percentage, in which case LNG composition should be known to determine the amount of slipped methane. Pavlenko et al. (2020) also mention reporting of methane slip as mass of methane per volume of LNG or per the energy content of the available fuel. In this report, the methane slip is expressed in brake specific basis, as mass of methane per useful shaft work of the engine (g/kWh), enclosing the efficiency of the engine. This was also the most common method of reporting found in the included literature. In the cases where methane emissions were expressed as CO_2 equivalents (gCO_2eq/kWh), the 100-year CO_2 equivalent of 36 used in the specific study (Balcombe et al., 2022) was used for conversion.

4.2. Methane emission factors

4.2.1. Methane slip from different sized engines

For LPDF 4-S and 2-S engines, emission factors as function of engine power are shown in Figure 4 and Figure 5. For LBSI engines, 7 engines were included in the study by Ushakov et al. (2019) but engine size was included for only one of the engines (1.46 MW), for which emission factors ranged from 3.7-27.6 g/kWh. For HPDF engines no values related to engine size were found.

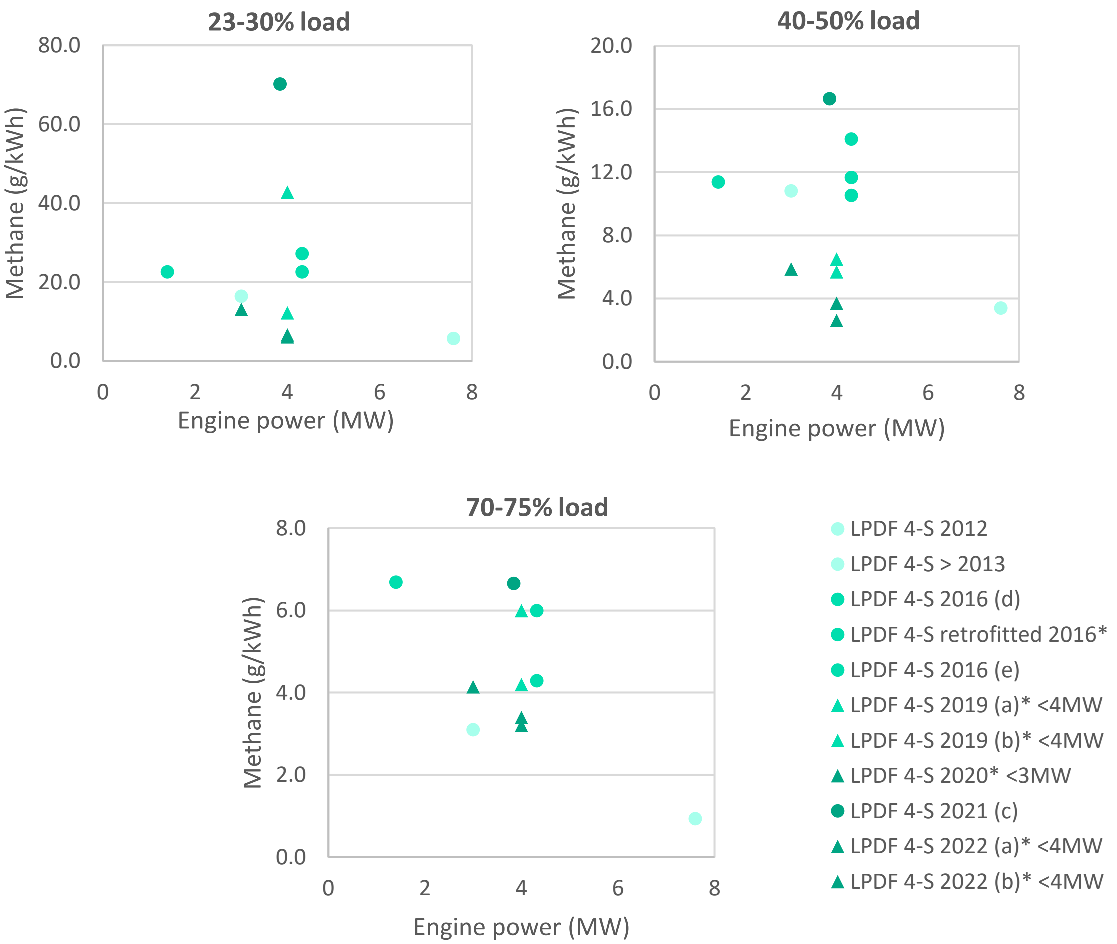

Figure 4. Methane emission factors reported for LPDF 4-S engines with varying engine sizes at 23-30%, 40-50%, and 70-75% load points. Darkest tones are used for engines from years 2020-2022, midtones for engines from years 2016-2019 and light tones for engines from years 2015 or older. Measurements conducted in testbed are marked with asterisk. It should be noted that in cases, when exact engine size is not known (triangles), range (e.g. <4MW) is given in the label but result is plotted at the upper limit (e.g. 4MW).

For LPDF 4-S engines, emission factors were reported for engine sizes between 1.4-7.6 MW. Majority of reported values were between 0-30 g/kWh, but also increased values up to 270 g/kWh were observed, attributed to low load conditions as seen later in Figure 6 and Figure 7. Majority of the engines had maximum rated power below 4.3 MW with only one engine sized at 7.6 MW. At each load, lowest methane slip is seen for the 7.6 MW engine, but due to the single data point in this range and large variation between engines in the 3-4.3 MW definite conclusions of the effect of engine size are not possible. It should be noted that for part of the engines, only upper limit of the engine size range is known (triangles in Figure 4) and thus smaller engine size may be one explanation to the variation in emission factors seen at 23-30% load and 40-50% load. In the category of engines below 4MW, the new engines from 2020-2022 give the lowest emissions of 3.2-4.1 g/kWh together with the LPDF 4-S engine from 2012.

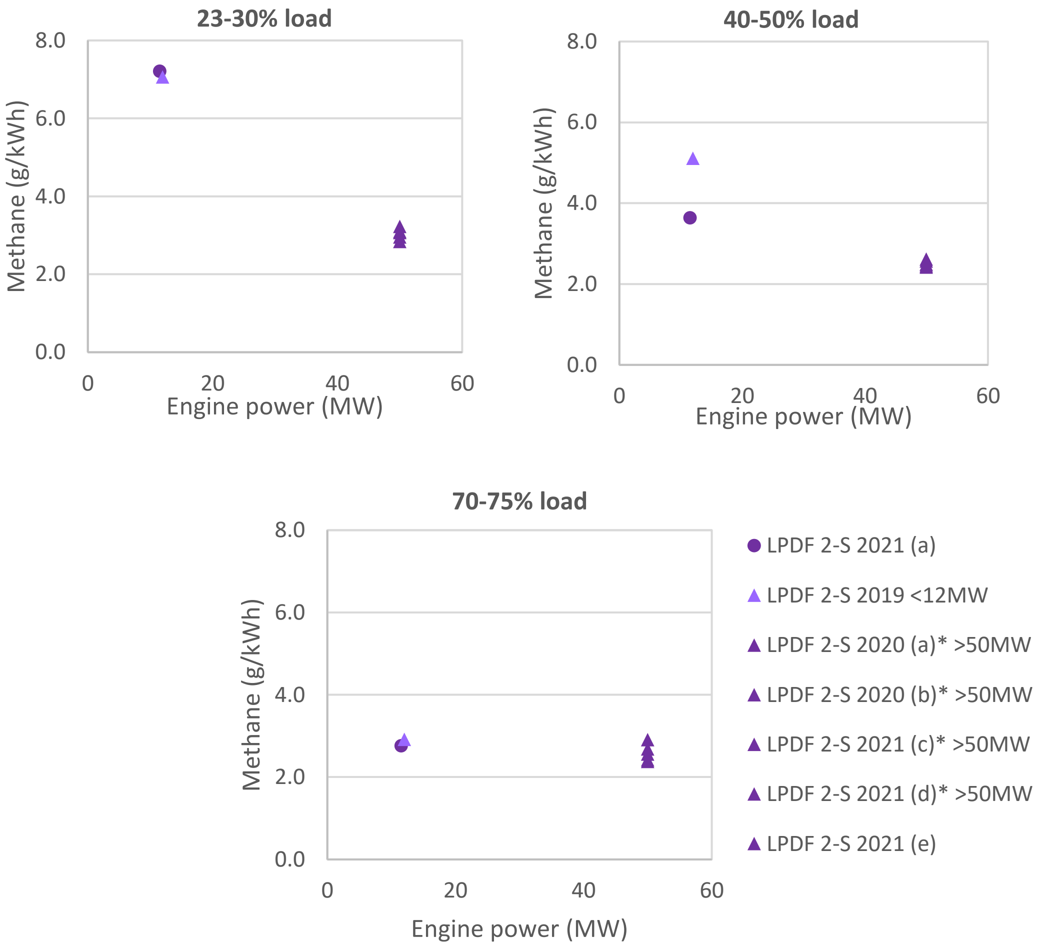

Figure 5. Methane emission factors reported for LPDF 2-S engines with varying engine sizes at 23-30%, 40-50%, and 70-75% load points. Darkest tones are used for engines from years 2020-2022 and midtones for engines from years 2016-2019. Measurements conducted in testbed are marked with asterisk. In cases, when exact engine size is not known (triangles), range (e.g. <12 MW) is given in the label but result is plotted at the given limit (e.g. 12 MW).

For LPDF 2-S engines, emission factors were found for engine sizes of 11.53 MW, <12 MW and > 50 MW. Methane slip emissions were mainly between 2.4-3.6 g/kWh, but emissions at low load point as seen later in Figure 6 and Figure 7 could range up to 7.2 g/kWh. Generally, the load dependent variation in methane slip emission factors seems to be suppressed in larger engines, where each load condition gave emission factors between 2.5-3.1 g/kWh. Overall, the variation among methane slip at certain load and engine size is smaller for LPDF 2-S engines, possibly because these engines are from recent years and likely from a single manufacturer. In comparison to LPDF 4-S engines, LPDF 2-S produce lower methane slip, especially at lower loads.

4.2.2. Methane slip as function of engine load

4.2.2.1. Brake specific emission factors

Methane slip emission factors as a function of engine load were most often reported as brake specific emission factors (g/kWh). Figure 6 shows the methane slip values for 7 LBSI 4-S engines, 14 LPDF 4-S engines, and 7 LPDF 2-S engines. For LBSI engines, emission factors were found for engine loads between 10 and 100% whereas in the case of LPDF 4-S engines, values were found for 0-100% loads and in the case of LPDF 2-S engines for 25-100% loads. For HPDF engines, no load specific values were found. However, a recent report gave methane emission factor ranges of 2.4-5.8 g/kWh for LPDF 4-S engines with engine load above 50%, and 1.6-2.3 g/kWh for LPDF 2-S engines without EGR, 1.1-1.6 g/kWh for LPDF 2-S with EGR, and 0.2-0.28 g/kWh for HPDF 2-S engines for engine load ranges between 25-85% (Mærsk Mc-Kinney Møller Center for Zero Carbon Shipping, 2022).

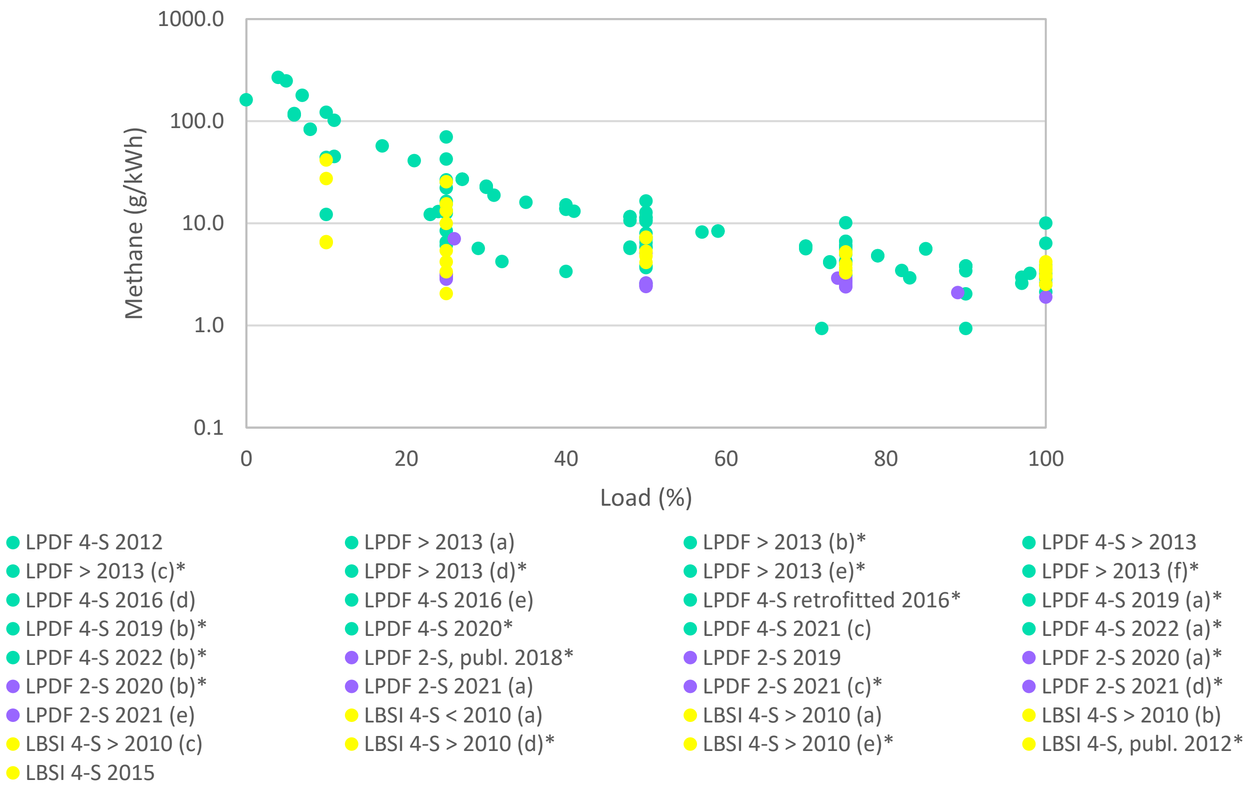

Figure 6. Methane emission factors as a function of engine load for all engine types. Green color scale is used for LPDF 4-S engines, purple for LPDF 2-S engines and yellow for LBSI 4-S engines. Measurements conducted in testbed are marked with asterisk. If engine year is not available, publication year (indicated by 'publ.') is used instead. Note logarithmic scale.

Increase in brake specific methane emissions as function of decreasing engine load can be observed with all engine types. For LBSI 4-S engines at 100% load, emission factors range between 2.5-4.2 g/kWh when the range at 75% load is 3.3-5 g/kWh, at 50% load 4.1-7.2 g/kWh and at 10% load 6.4-42 g/kWh. Respectively, for LPDF 4-S engines (shown separately in Figure 7), the ranges are 2.6-10.0 g/kWh at 100% load, 3.1-10.1 g/kWh at 75% load, 2.6-16.7 g/kWh at 50% load, 6.1-70.2 at 25% load and 12.2-123 g/kWh at 10% load. Again, in the case of LPDF 2-S engines (Figure 7), reported emission factors for between 1.9-2.5 g/kWh for operation at 100% load, 2.4-2.9 g/kWh at 75% load, 2.4-5.1 g/kWh at 50% load and 2.8-7.2 g/kWh at 25% load.

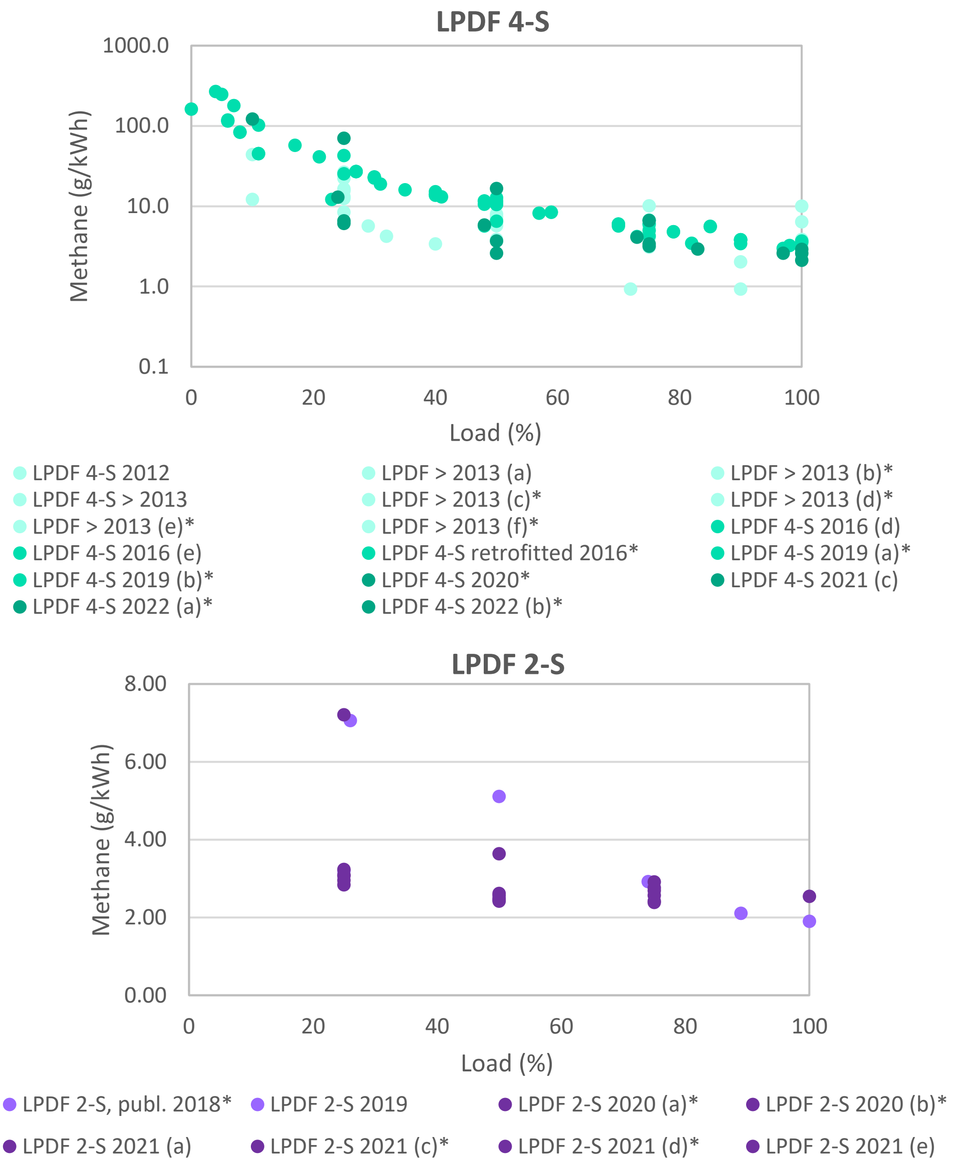

Figure 7. Methane emission factors as a function of engine load for LPDF 4-S and LPDF 2-S engines. Darkest tones are used for engines from years 2020-2022, midtones for engines from years 2016-2019 and light tones for engines from years 2015 or older. Measurements conducted in testbed are marked with asterisk. If engine year is not available, publication year (indicated by 'publ.') is used instead. Note logarithmic scale in the upper figure.

The engines were classified in three categories representing the newest engines from years 2020-2022, engines from years 2015-2019 and engines from year 2015 or older (indicated with different tones in figures above). For the newest engines, data originated either from ship owner or the recent study by (Balcombe et al., 2022) whereas for the engines before 2015 data originated mainly from the study by (Anderson et al., 2015) and the data set presented by Stenersen & Thonstad (2017) and Ushakov et al. (2019). The engines presented in the latter set of data as post-2013 were labeled to be in the 2015 or older category since the exact year is not known, however they could be from 2016 or 2017, the year of the first publication. Methane slip for engines from different years is discussed further in section 4.2.4.

4.2.2.2. Low load points and mitigation strategies

Increasing methane slip at low engine loads is visible in Figures 6-7 and attention to the phenomenon was also given in the publications (Peng et al., 2020; Sommer et al., 2019) where the effect of methane slip at low loads to GWP was discussed and one low-load mitigation strategy investigated.

In the study by Sommer et al. (2019), emissions were reported from two dual-fuel engines of the same engine model, where one of the engines used cylinder deactivation as a strategy to decrease methane slip at low loads. The results from the study are reproduced in Figure 8 where it is shown that cylinder deactivation could markedly reduce the methane slip at low loads. During the study, the engine marked here as LPDF 4-S 2016 (d) used unmodified firing strategy (all cylinders firing at all loads) whereas the engine LPDF 4-S (e) used a modified strategy to deactivate 3 cylinders at loads below 15%.

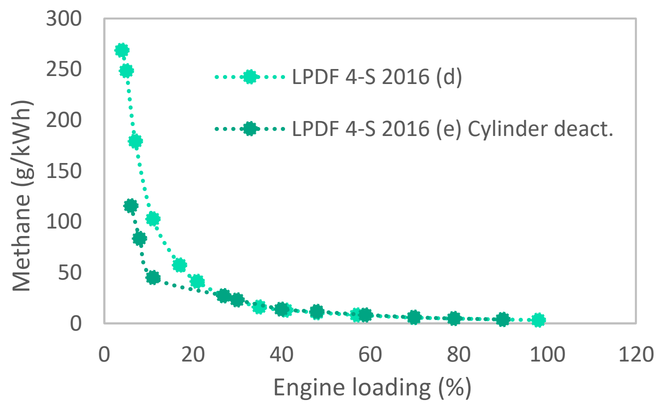

Figure 8. Effect of cylinder deactivation on methane slip. Figure reproduced based on data from the publication of Sommer et al. (2019)

The increased methane slip has been shown to have high impact on the GWP of emissions from LNG operated engine at low loads. Peng et al. (2020) noted that while methane accounts the greatest fraction of GWP at low loads, its contribution significantly decreases as engine load increases, being largely reduced at load conditions above 75% which underlines the importance of methane slip mitigation at low loads or avoiding operation at low loads entirely. It is understood that often, at low loads, dual-fuel engines switch to using liquid fuel as was reported in the study by Anderson et al. (2015) at 16% load point. Other mitigation strategies may include avoiding low load operation e.g. by using hybrid propulsion combining engines with batteries or by using shore power at berth as mentioned in the study of Sommer et al. (2019).

4.2.3. Weighted emissions E3/E2 cycle

In part of the publications, methane slip values were found expressed as the weighted emission factors over the ISO 8178 E3/E2 test cycle used for reporting NO_x emissions. In cases where emission factors for load points 25, 50, 75, and 100% were given, the weighted emission factor was also calculated for other data sets and synthesized results are shown in Figure 9. It should be noted that in cases where data was not given directly (marked as 'Estimate'), g/kWh emission factors at different load points were used for the calculation which introduces small error compared to dividing weighted emissions by the weighted work. This however gives an overall idea of the variability among different studies.

For LBSI engines, the weighted emission factors ranged between 2 and 5.5 g/kWh, with lowest value given for new engines (data from different manufacturers, Schuller et al., 2021). In case of LPDF 4-S engines, the weighted emissions are 2-13.5 g/kWh, majority of values being between 3.3-6.9 g/kWh. For newest engines, on-board study (Balcombe et al., 2022) results 13.5 g/kWh whereas data from testbed engines results 3.7-5.4 g/kWh. Considering LPDF 2-S engines, three values from shipowner data could be calculated, resulting in 2.1-3.5 g/kWh. For HPDF 2-S engines, one value of 0.23 g/kWh was found (Schuller et al., 2021) with other studies giving similar ranges of 0.2-0.3 g/kWh (Lindstad et al., 2020) and 0.2-0.28 at 25-85% load (Mærsk Mc-Kinney Møller Center for Zero Carbon Shipping, 2022) without specifying if the value is weighted.

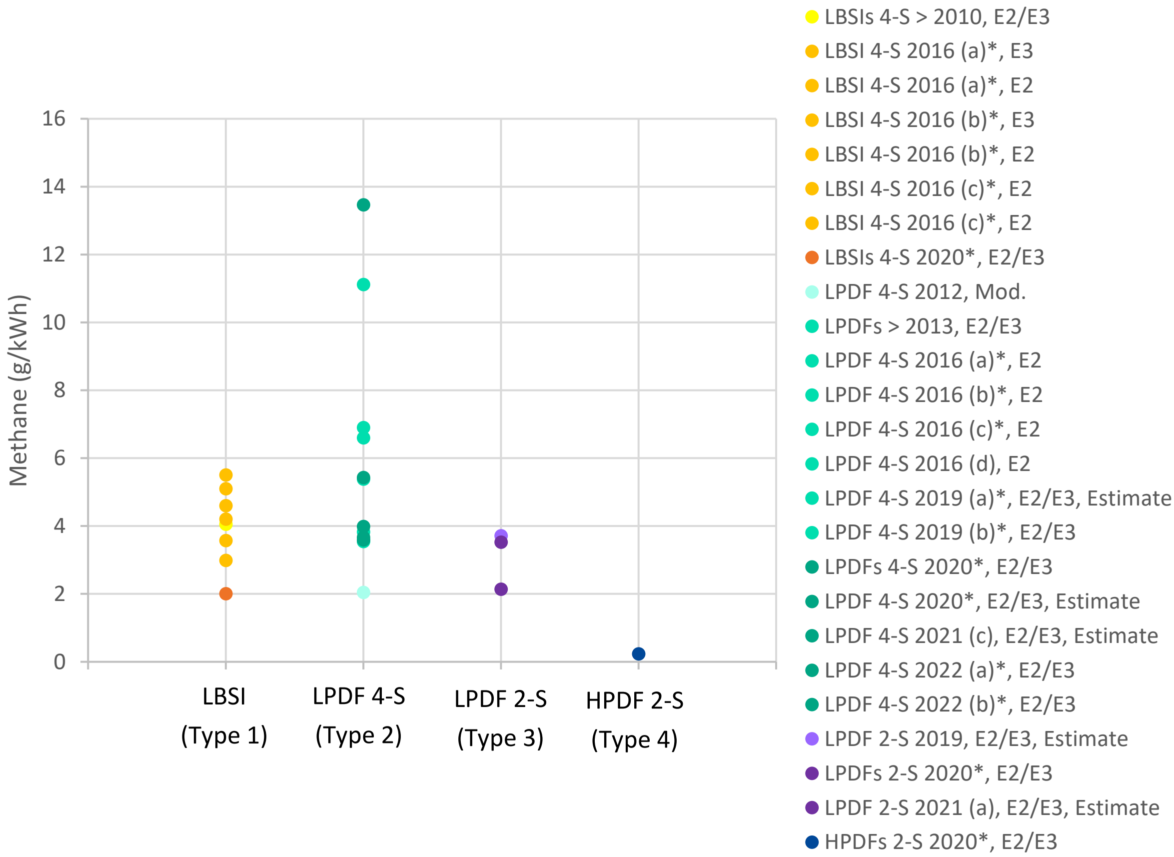

Figure 9. Methane emission factors calculated according to E2 or E3 cycles where load conditions of 100%, 75%, 50%, and 25% are weighted with factors of 0.2, 0.5, 0.15, and 0.15. In the case of LBSIs 4-S 2010, data from 7 engines is synthesized to calculate the emission factor, as well as in the case of LPDFs > 2013, where stroke is not specified for all engines (Ushakov et al., 2019). *In case of LPDF 4-S 2012, Mod., loads of 90%, 72%, 40% and 29% were used for calculation* (Anderson et al., 2015).

The use of E3/E2 test cycle in reporting of methane slip was also debated in some of the publications. For example, Lindstad et al. (2020) presented that today's vessels typically operate at less than 75% power, suggesting that the use of E2/E3 cycle may underestimate the methane slip compared to real-life operation. Based on STEAM model data for year 2021, the average main engine load for ships using LNG engines is 60.5%. In their study, Peng et al. (2020) reported methane slip emissions weighted over the E2 cycle but also over actual ship activity profile for a vessel that was operated in harbor service, not at open sea. They noted that by considering the actual operation conditions of the vessel, where long time periods are spent at idle, the actual weighting factors that should be used to depict the operation of the specific vessel (idle 0.32, 25% 0.09, 50% 0.06, 75% 0.31, 100% 0.22) were significantly different from the E2 cycle and for that reason, the emission factors of methane and total hydrocarbons weighted according to the E2 cycle resulted in 40% lower values than when actual operation weighting factors were utilized. It seems that to understand methane slip emissions from varying vessel types with different activity profiles, reporting load specific emission factors which then can be used together with an activity profile of a certain ship would be most preferable.

Also, it should be noted that the transient conditions such as acceleration and deceleration are not considered in the E3/E2 cycles. In automotive and off-road industry, transient loads and various operating variable conditions are included in the test cycle (e.g. WLTC cycle for EuroVI regulation). Still largely not investigated for marine engines, this topic is expected to gain interest in the future, as transient conditions may significantly degrade engine performance and could produce additional methane-slip.

4.2.4. Methane slip from engines from different years

Methane slip for LPDF 4-S and LPDF 2-S engines as function of engine year at 23-30%, 40-50%, and 70-75% loads are shown in Figure 10 and Figure 11. For LPDF 4-S engines, the reported methane slip emission factors for engines from 2016-2019 agree or surpass those from older engines at all engine loads. For the newest engines, the gathered results give twofold trend; the emission factors obtained from ship owner data from testbed measurements show decreased methane slip compared to older engines whereas the on-board study by (Balcombe et al., 2022) presents levels clearly exceeding the previous values especially at loads of 25-50%. For the newest engines, ship owner data gives 2.6-2.9 g/kWh at 100% load, 3.4-4.1 g/kWh at 73-75% load and 6.6-13.05 g/kWh at 25% load, when the reported on-board values are appr. 2 g/kWh at 100% load, 7 g/kWh at 75% load, 17 g/kWh at 50% load, 70 g/kWh at 25% load and 123 g/kWh at 10% load. Differences in these values affecting the conclusions that can be drawn about engine construction year may originate from operational differences in testbed and on-board as well as different measurement methodology and accuracy and possibly comparing engines from different manufacturers which may utilize varying technological solutions.

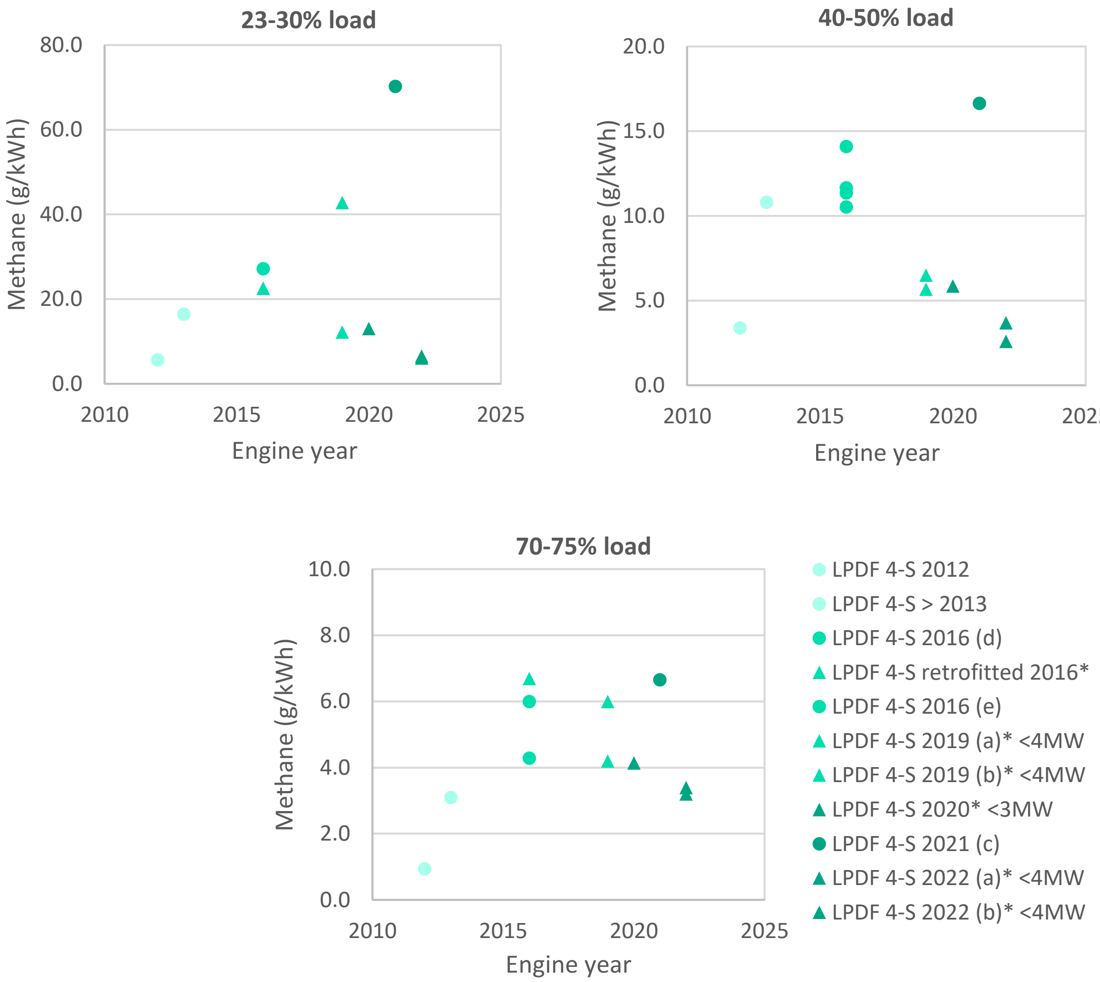

Figure 10. Methane emission factors as function of engine year for LPDF 4-S engines at 23-20%, 40-50%, and 70-75% loads. Darkest tones are used for engines from years 2020-2022, midtones for engines from years 2016-2019 and light tones for engines from years 2015 or older. Measurements conducted in testbed are marked with triangle and labeled with asterisk.

Considering LPDF 2-S engines, most of the obtained data is from new engines, with one dataset reported for engine from 2019. Again, either ship owner data from on-board measurements or testbed is available, together with the on-board study by Balcombe et al. (2022). Comparing the testbed and on-board results to on-board measurement on 2019 engine, the ship owner data again suggests decrease in methane slip with newer engines except in the case of 23-30% load where the results from (Balcombe et al., 2022) report slightly increased levels. However, these reported values are in much better agreement with more than 2-fold difference at 23-30% load compared to the case of LPDF 4-S engines where almost 5- to 11-fold difference is observed at 23-30% load. This may partly reflect the higher number of data and different engine manufacturers in case of LPDF 4-S engines. However, the shipowner data for new engines shows that methane slip can reduced with the newer engine technology and these new data should be considered when current methane emissions from LNG engines are evaluated.

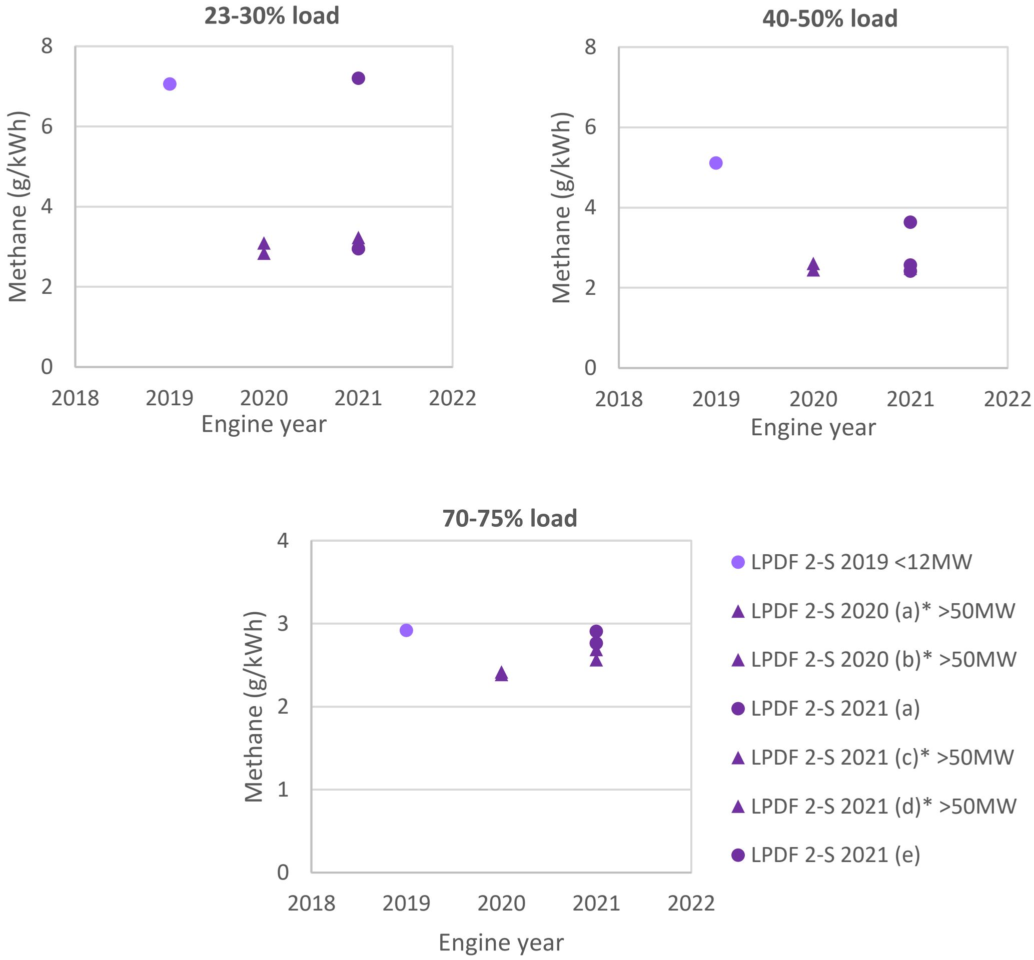

Figure 11. Methane emission factors as a function of engine year for LPDF 2-S engines at 23-30%, 40-50%, and 70-75% loads. Darkest tones are used for engines from years 2020-2022 and midtones for engines from years 2016-2019. Measurements conducted in testbed are marked with triangle and labeled with asterisk.

4.2.5. Comparison of on-board and testbed measurements

Figure 12 shows the data from Figure 7 grouped by the measurements conducted on-board and in testbed. In their study, Ushakov et al. (2019) reported methane emissions from same model LPDF engines in laboratory and at sea and noticed a 32% increase between on-board measurement compared to manufacturer values. They assumed the difference to be partially explained by differences in engine conditions in laboratory and at sea. Considering all the data for LPDF 4-S engines, reasonable agreement is seen between the values from testbed measurements and those reported from on-board campaigns at 100%, 75%, 50%, and 25% loads. Only one value based on manufacturer values from testbed measurements was found for loads below 23%, which makes comparison difficult, although agreeing with the on-board measurements.

For LPDF 2-S engines, less data is available overall, but it can be noticed that methane slip for <12MW LPDF 2-S engine from 2019 and 11.53MW LPDF 2-S engine from 2021 (Balcombe et al., 2022) show increased methane slip compared to the testbed measurements. However, the on-board results for the LPDF 2-S 2021 of the same size category (>50MW) as the testbed engines agrees well with the testbed results, indicating that in the case of data presented here, engine size may have larger impact than the operation environment.

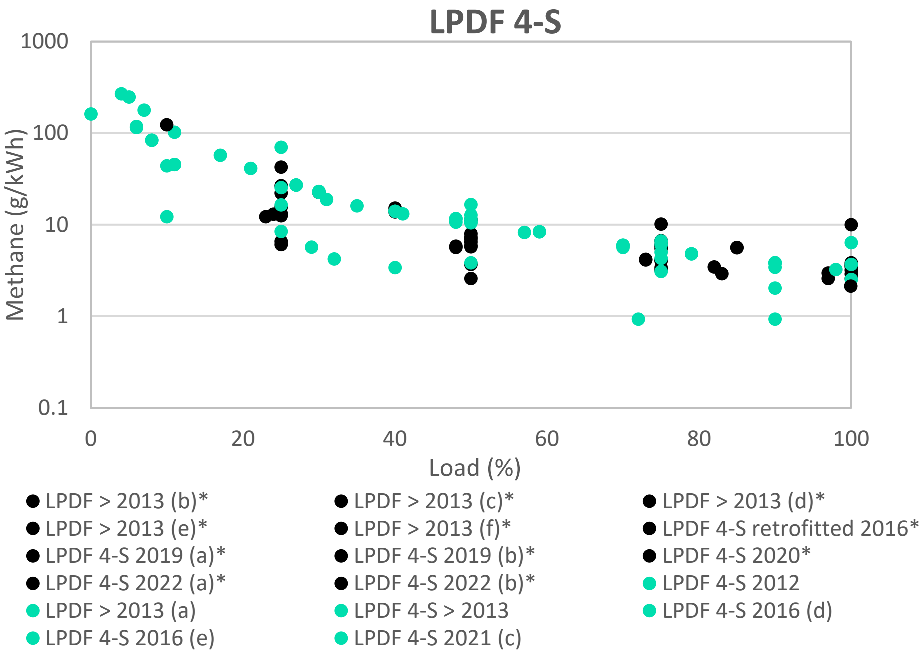

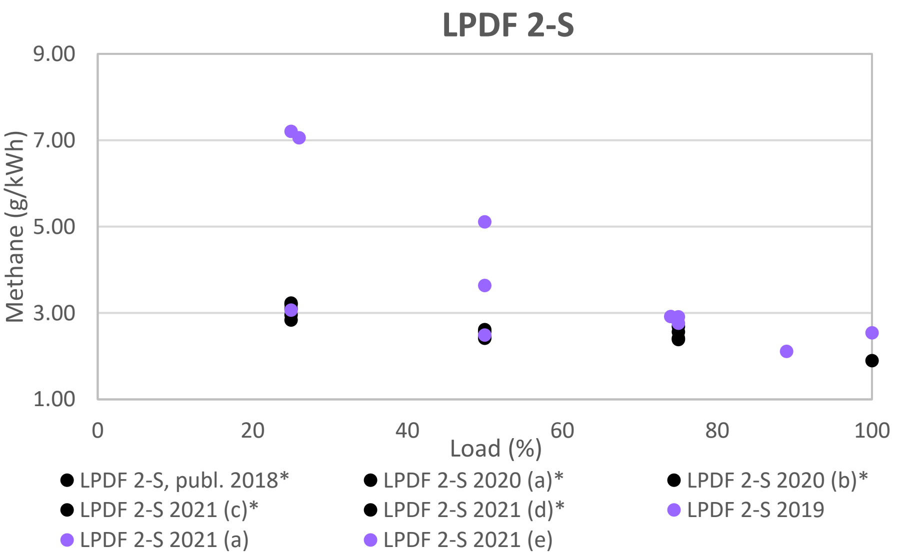

Figure 12. Methane slip emission factor for LPDF 4-S (top) and LPDF 2-S (bottom) engines measured in testbed (in black) or on-board (in green / purple). Note logarithmic scale for LPDF 4-S. In the case of LPDF 4-S 2021 (c), measurements were conducted on-board for 25-75% loads, but 10% and 100% are based on manufacturer data.

For LBSI engines, testbed and onboard data could be compared only from the study by Ushakov et al. (2019) and figure is not reproduced here. Referencing their findings, they found that testbed and on-board measurement of a same engine model showed rather good agreement at loads above 50% but a discrepancy was observed at lower loads with 400% difference at 25% load. Differences maybe caused due to more challenging engine conditions at sea or comparing engines from different manufacturers. Factors affecting the difference between laboratory and on-board measurements may be operating the engine at stable load without fluctuations, using gas with controlled composition within specification, clean injectors, and combustion chamber whereas changing conditions at-sea may include varying engine loads and conditions (Ushakov et al., 2019).

In most studies, methane slip emissions were given as brake specific emission factors, but in the study of Balcombe et al. (2022), for several engines, methane slip was given for varying load points as percentage of slipped methane out of the total fuel consumption. These results add to the information that can be found related to on-board studies. For comparison, methane slip as percentage was calculated from ship owner data sets where fuel consumption data was available. In total, these data sets covered the post 2019 engines included in the study. In Figure 13, it is seen that in the case of LPFD 2-S engines, the percentual methane slip varies between 0.03-5.3% at load between 10-90%, but also higher values of 8 and 15.6% are seen at 8 and 10% loads. Balcombe et al. (2022) also observed the methane slip at low loads to vary from two same model LPDF 2-S engines. The methane slip from LPDF 2-S reported from on-board measurements (Balcombe et al., 2022) and from testbed and on-board measurements (ship owner data) are consistent.

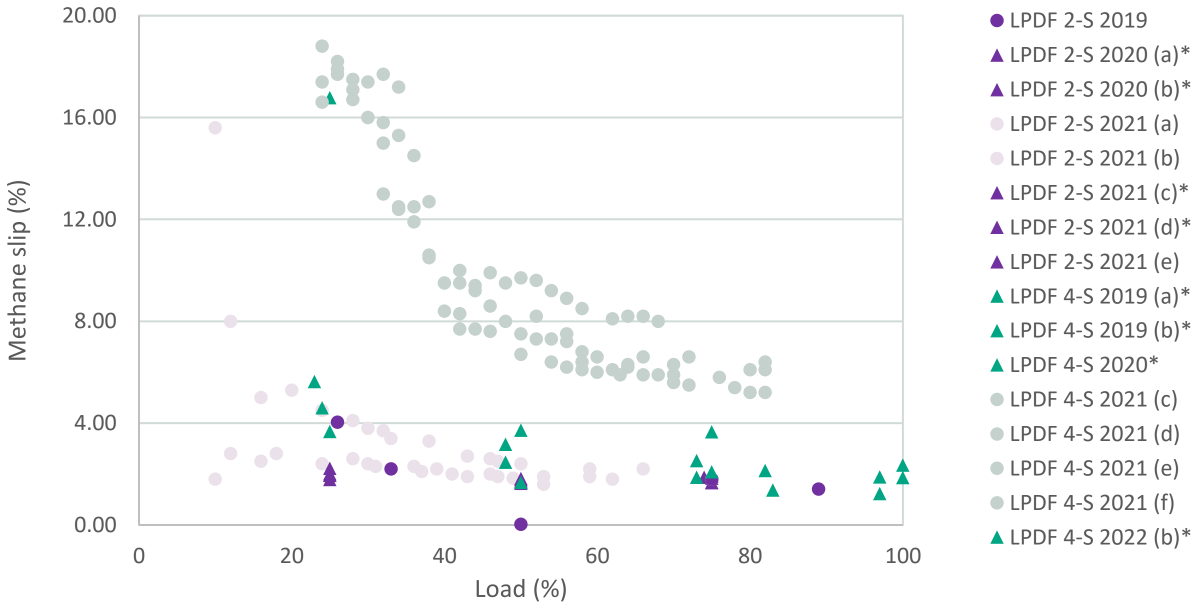

Figure 13. Methane slip emissions given as percentage of fuel use, as a function of engine load. For LPDF 4-S engines, light grey circles mark data from on-board (Balcombe et al. 2022) and dark green triangles mark ship owner data measured in testbed. For LPDF 2-S engines light purple dots mark data from on-board study (Balcombe et al. 2022), dark purple dots mark ship owner data measured on-board and dark purple triangles ship owner data measured in testbed.

For LPDF 4-S engines, the data from testbed measurements indicate that less than 5.6% of methane is released from the engine unburned, at load conditions of 23% and higher. The measurements on-board (Balcombe et al., 2022) show higher slips of below 10% at loads exceeding 40% but even 18.8% slip at 24% load condition. Generally, in case of LPDF 4-S engines, there is discrepancy between the testbed and on-board data, however one value from test-bed measurements at 25% load for engine from 2019 also shows slip of 16.6% indicating that higher slip may occur also in testbed conditions.

4.3. Other emissions from LNG engines

In addition to methane, information of other emissions of gaseous and particulate pollutants from LNG engines were collected. It must be noted, that here only publications which also reported methane slip are included and thus this chapter is not a full review of all other emission species that could be found in the literature. Most commonly, NO_x and CO_2 emissions were reported in parallel with methane slip, but also emission factors for other gaseous emissions (Appendix B) of carbon monoxide (CO), total hydrocarbons, and non-methane hydrocarbons (NMHC) as well as for formaldehyde (HCHO) were found. Particle emissions (Appendix C) were reported in different quantities; total particle mass or number (PM_{tot}, PN_{tot}), non-volatile particle mass or number (PM_{nv}, PN_{nv}, measured either according to ISO 8178 or PMP protocol, or by using thermodenuder or catalytic stripper to remove volatile compounds), elemental and organic carbon (EC, OC), or black carbon (BC).

CO_2 emission factors were included for three LPDF 4-S and one LPDF 2-S engine. Two of the LPDF 4-S engines showed relatively similar values of 394-420 g/kWh at 72-90% load and 451-485 g/kWh at 29-40% load whereas for one engine the emission curve was shifted to higher values of 500-530 g/kWh at 75-100% load and 580-660 g/kWh at 25-50% loads, respectively. For this engine, results at low load of 10% were reported, showing increased value of appr. 1100 g/kWh, suggesting worse fuel economy at low loads. Results for the LPDF 2-S engine were reported for loads between 25% and 100% and showed minimal load dependency in this range with CO_2 emission varying between 397-422 g/kWh with lowest value at 75% load and highest at 25% load.

Emissions of nitrogen oxides (NO_x) were found for 10 LPDF 4-S engines and 8 LBSI 4-S engines. For the LPDF 4-S engines, the NO_x emission factors vary between 0.5-4.3 g/kWh. In general, the emission factors follow a U-shaped curve with lowest values at 75% load, but in two cases (LPDF > 2013, (a-b)), rather N-shaped curve was noticed with lowest values at 75% load and 10-25% but higher values exhibited at 50% load. NO_x emission factors for the LPDF 4-S engines were 0.5-2.8 g/kWh at 75% load, 0.6-3.8 g/kWh at 50% load and 1.1-2.6 g/kWh at 25% load. For LBSI 4-S engines, emissions of 0.26-3.3 g/kWh were found at loads between 25-100%, but in two cases, clear load dependency was observed, resulting in emission factors of 15-27 g/kwh at 10-25% loads. For medium speed engines, the IMO Tier II and Tier III weighted emission limits introduced in 2011 and 2016 (for SECA areas) are dependent on engine's rated speed and are for example 9.7 g/kWh and 2.4 g/kWh for engines with rated speed or 720 rpm (IMO, 2022c). Majority of the reported LPDF engines achieved the Tier III values and in the on-board measurement from engines from 2012 and 2016, NO_x emissions from all load points between 25-100% were between 0.5-1.1 g/kWh. In the study of Ushakov et al. (2019) possible overtuning of engines for very low NO_x emissions was discussed as one reason for higher methane slip, underlining the importance of balancing between low NO_x and low methane emissions.

Carbon monoxide (CO) and unburned hydrocarbons (measured as total hydrocarbons including methane, THC, or non-methane hydrocarbons, NMHC) are products of incomplete combustion. Peng et al. (2020) observed simultaneous increase of CO and hydrocarbons together with methane in conditions where NOx decreased and indicated the higher emission factors of the incomplete combustion products to be caused by imperfect flame propagation in uneven-temperature regions of combustion chamber. In the included literature, CO emissions were reported for 3, THC emissions for 2, and NMHC emissions for 1 LPDF 4-S engine. The CO emission factors varied between 1-7 g/kWh at 25-100% load with increased values at lower loads. For one engine, emission of 36.3 g/kWh was reported at idle. Also THC increased towards low loads, with emission factors varying between 1.1-6.7 g/kWh and 4.4-31 g/kWh for the two engines from 2012 and 2016, respectively, at loads between 100% and 25%. For the second engine, 188 g/kWh was reported during idling. The reported emissions for hydrocarbons excluding methane were 0.57-2.9 g/kWh, also increasing towards decreasing loads between 100% and 25%, and value of 20.6 g/kWh being reported at 6% load.

Some studies (Lehtoranta et al., 2017; Peng et al., 2020) also considered emissions of formaldehyde (HCHO). Despite the lower levels of most air pollutants from natural gas engines compared to diesel engines, formaldehyde is a carcinogenic oxidation product to be monitored from LNG engines. Formaldehyde is an early interstage product of the methane oxidation which starts its formation at low temperatures but gets fully oxidized only above a certain minimum temperature level (800-900°C). Cold regions in the combustion chamber have been reported as the main sources of formaldehyde emissions and it is stated that generally the amount of formaldehyde emissions increases with the amount of unburned methane. (CIMAC WG 17, 2014). In their study, Peng et al. (2020) found formaldehyde emissions of 124-466 mg/kWh when engine load decreased from 100% to 25%. At idle, 2 520 mg/kWh of formaldehyde was produced, indicating incomplete combustion at such low load condition. Lehtoranta et al. (2017) presented formaldehyde in ppm units, but corresponding emission factors could be received from VTT database, showing lower values of 210-700 mg/kWh at loads decreasing from 85% to 30%. Comparing to the same engine operating with diesel fuel in the study by Peng et al. (2020), formaldehyde emissions of 16-32 mg/kWh (loads 100% to 25%) and 337 mg/kWh at idle were reported, almost one magnitude lower than for natural gas, pinpointing the importance of considering formaldehyde in addition to methane when developing the technology of LNG engines.

Natural gas typically contains very low amounts of sulfur, but sulfuric compounds may be added as odorants. More significant source of sulfur in dual-fuel engines is the diesel used as pilot fuel, although the total SO_2 concentration remains low, even posing a challenge for its measurement. In the included literature, no values for SO_2 emissions in the exhaust of natural gas combustion were found, although Lehtoranta et al. (2019) observed lower than 2 ppm concentration for full marine gas oil operation and indicate even lower concentration with dual-fuel operation with natural gas. Although the emissions of sulfur dioxides are low from natural gas engines, making them suitable at operation in emission control areas, even low concentrations of sulfur in the exhaust may pose a challenge for the use of methane oxidation catalysts. One mitigation option could be the use of ultra-low sulfur diesel (ULSD) as pilot fuel.

Particle emissions from natural gas engines were included in part of the studies (Anderson et al., 2015; Corbin et al., 2020; Lehtoranta et al., 2019; Peng et al., 2020), in addition, PN and PM emissions were included from the study of Alanen et al. (2020) who considered the same retrofit engine as Lehtoranta et al. (2019). Total particle mass emissions varied between 0.15-2.6 mg/kWh (10-173 mg/kWh at 6% load), 0.16-0.41 mg/kWh, and 7-11 mg/kWh for the three engines included, indicating significant variation is possible between different engines. Non-volatile particle mass emissions of 0.14-0.22 mg/kWh and 10-32 mg/kWh were also reported for the second and third of the abovementioned engines, measured either by converting particle number size distribution measured downstream thermal denuder to mass or by collecting particle matter on a filter according to ISO 8178 protocol, respectively. Whereas variation between the engines is shown, the different measurement method may also cause part of the variation. However, for the same retrofit engine, the total PM measurement by number size distribution method gave results (7-11 mg/kWh) with better agreement to the filter method (10-32 mg/kWh).

Particle number emissions have also been reported either as total or non-volatile particle number for four LPDF 4-S engines. In principle, total particle number considers also particles born by nucleation of semi-volatile vapors in the exhaust duct or during dilution, whereas non-volatile particle number considers primary soot spherules and agglomerates as well as ash originated particles with solid nature in exhaust gas temperatures. The reported non-volatile PN emissions from different studies were 1.3×10^{11} 1/kWh (>23nm), 1-1.1×10^{12} 1/kWh (>23nm), 1.0-3.0×10^{12} 1/kWh (>5.6nm) without notable load dependency in the case of three of the engines, but in one case also high load dependency is observed with PN_{nv} emissions of 1.7-3.0×10^{12} 1/kWh (>6nm) at 53-90% loads but emissions being increased by over two orders of magnitude to 1.0-3.0×10^{15} 1/kWh (>6nm) at low loads of 6-31%. For total particle number, load dependency was not clear but the three engines for which values were reported differed from each other with PN emission factors in the range of 2.3-6.9×10^{12} 1/kWh (>5.6nm), 0.18-2.7×10^{15} 1/kWh (>6nm), and 3.0-4.0×10^{15} 1/kWh (>1nm).

Some of the variation in the PN_{tot} and PN_{nv} results could be caused by the lowest cut-off point of the used PN instrument. The cut-off varied in the studies from 1 nm to 23 nm determining how small particles are counted and is therefore indicated in parentheses for the results. However, for example in case of the total PN, there is great variation in results from engines where instruments with cut-off points of 5.6 nm and 6 nm, very close to each other, were used. In the study by Alanen et al. (2020), the aid of transmission electron microscopy imaging was used to identify four different particle types in the exhaust of dual-fuel natural gas engine; soot agglomerates, nucleated particles from semi-volatile vapors, non-volatile core particles originated from lubrication oil, and core particles originated from the pilot fuel. From their study, it was observed that majority of non-volatile PN from LNG engine may reside well below the 23 nm cut-off point defined by the PMP method. In the recent proposal for EURO 7 emission regulation considering on-road vehicles, the lowest cut-off point in PN measurement is brought down to 10 nm (European Commission, 2022). All in all, it can be seen from the results that low PN levels of 10^{11} kWh^{-1} can be achieved using LNG engines, but the PN emissions are not necessarily low, and depend on the specific engine and its condition, load, pilot fuel and lubrication oil used.

Emissions of black carbon as well as elemental carbon (analyzed together with organic carbon) were included in two studies for LPDF 4-S engines, where BC or EC emission factors varied between 0.5-1.7 mg/kWh at loads between 25-100% but reached higher values of 5.7-5.9 mg/kWh at 6% load and 6 mg/kWh at idle. Black carbon is recognized among the three most important anthropogenic climate warming compounds together with carbon dioxide and methane. Reported together with EC, organic carbon emission factors were 2.3-25.3 mg/kWh at loads between 25-100% but they again showed increased values from 9 to up to 1450 mg/kWh at 6% load and 110 mg/kWh being reported at idle. The ratio of organic carbon to elemental carbon varied between 1.8-18.3. The BC, EC, and OC emissions from the dual-fuel natural gas combustion were on a low level as for example Peng et al. (2020) observed combustion of ULSD diesel to result in values of 14.9-38 mg/kWh for EC and 85-151 mg/kWh for OC at 25-100% loads.

Peng et al. (2020) further compared the effects of switching a dual-fuel marine vessel from diesel to natural gas operation. They found that the use of natural gas reduced emissions of NO_x, $PM_{2.5}$, CO_2, and BC by 92%, 93%, 18% and 97%, respectively. Similarly, Lehtoranta et al. (2019) found PM to decrease 72-75% and PN_{nv} by 98-99% when comparing LNG use to marine diesel oil. In a recent review Aakko-Saksa et al. (2023, Fig. 6), LNG combustion in DF engines showed significant reduction for PM emissions but also for PN and BC emissions compared to liquid fuels. The reductions on criteria pollutants have been noted as significant in terms of improving air quality in coastal areas where great fraction of these pollutants originate from shipping. However, in the study of Peng et al. (2020), parallel to higher methane emissions, caused by fuel switching, the emission factors of CO and formaldehyde (HCHO) increased more than fivefold and sevenfold, respectively. The reduction of PM from natural gas combustion compared to diesel during idling at port was associated with 92% lower cancer risk on the long term, whereas higher formaldehyde emissions from natural gas could remain a concern and possibly require mitigation by catalytic aftertreatment (Peng et al., 2020).

5. Conclusions

The use of liquefied natural gas as maritime fuel has increased but is still marginal: less than 3% of ships that reported to the EU MRV in 2021 had a carbon factor less than 3.0, which is an indication of alternative fuel use and most likely LNG. The share of LNG of total annual fuel combusted on board ships was 5.9% in 2021 according to the IMO DCS. Methane will be part of future EU mechanisms to cut GHG emissions and mitigation of methane slip is needed to sustain the interest towards the use of LNG as marine fuel.

The amount of available methane slip information is limited with a handful of scientific studies reporting emission factors measured during on-board experiments. LPDF 4-S engines are best represented in the literature, followed by LBSI and LPDF 2-S engines. For HPDF engines, only values originating from manufacturers could be found but methane slip from these engines is considered low (0.2-0.3 g/kWh).

The emission factors reported for LBSI engines showed methane slip of 2.1-25.5 g/kWh at engine loads of 25-100%, indicating higher methane slip towards low loads. The LBSI engines that could be included were from years before 2010 until 2015.

For LPDF 4-S engines, the methane slip from newest engines from 2020-2022 measured in testbed varies between 2.6-4.1 g/kWh at 75-100% load but increased slip of 6.6-13.05 g/kWh is observed for 25% load. From on-board measurements, higher variation of 1.9-6.4 g/kWh at 75-100% loads and even 70.2 g/kWh at 25% have been reported. Differences in these values may originate from operational differences of the engine in testbed and on-board, different measurement methodology and accuracy as well as comparing engines from different manufacturers which may utilize varying technological solutions. Also, in the case of older engines, increased methane slip at low loads was observed. Methane slip remains a concern to be mitigated by the development of engine technology for new engines or by removal via exhaust aftertreatment. Cylinder deactivation was reported as one strategy to reduce methane slip at low engine loads.

For LPDF 2-S engines, data could be included for new engines from 2019-2022 and values of 1.9-7.2 g/kWh were found for engine loads between 25% and 100%. For the LPDF 2-S engines, reasonable agreement was observed between testbed and on-board studies.

Because load dependency for methane slip is observed, reporting emission factors as function of engine load instead of weighted emissions over the E3/E2 cycle would be beneficial in order to understand the methane emissions of ships with varying activity profiles of their engines, as well as for studying the influence of transient load conditions. In their study, Balcombe et al. (2022) noted that several continuous emission monitoring systems for methane are commercially available and would enable ships to self-monitor methane, helping further to understand and reduce the emissions. While the focus of this report is on Tank-to-Wake emissions, the comparison of different fuel and engine options should consider also upstream (Well-to-Wake) emissions (e.g. Balcombe et al., 2021; Lindstad et al., 2020; Schuller et al., 2021).

References

Aakko-Saksa, P. T., Lehtoranta, K., Kuittinen, N., Järvinen, A., Jalkanen, J. P., Johnson, K., Jung, H., Ntziachristos, L., Gagné, S., Takahashi, C., Karjalainen, P., Rönkkö, T., & Timonen, H. (2023). Reduction in greenhouse gas and other emissions from ship engines: Current trends and future options. In *Progress in Energy and Combustion Science* (Vol. 94). Elsevier Ltd. https://doi.org/10.1016/j.pecs.2022.101055

Alanen, J., Isotalo, M., Kuittinen, N., Simonen, P., Martikainen, S., Kuuluvainen, H., Honkanen, M., Lehtoranta, K., Nyyssönen, S., Vesala, H., Timonen, H., Aurela, M., Keskinen, J., & Rönkkö, T. (2020). Physical Characteristics of Particle Emissions from a Medium Speed Ship Engine Fueled with Natural Gas and Low-Sulfur Liquid Fuels. *Environmental Science and Technology*, *54*(9), 5376–5384. https://doi.org/10.1021/acs.est.9b06460

Anderson, M., Salo, K., & Fridell, E. (2015). Particle- and Gaseous Emissions from an LNG Powered Ship. *Environmental Science and Technology*, *49*(20), 12568–12575. https://doi.org/10.1021/acs.est.5b02678

Balcombe, P., Heggo, D. A., & Harrison, M. (2022). Total Methane and CO 2 Emissions from Liquefied Natural Gas Carrier Ships: The First Primary Measurements. *Environmental Science & Technology*. https://doi.org/10.1021/acs.est.2c01383

Balcombe, P., Staffell, I., Kerdan, I. G., Speirs, J. F., Brandon, N. P., & Hawkes, A. D. (2021). How can LNG-fuelled ships meet decarbonisation targets? An environmental and economic analysis. *Energy*, *227*. https://doi.org/10.1016/j.energy.2021.120462

CIMAC WG 17. (2014). *CIMAC Position Paper. Methane and Formaldehyde Emissions of Gas Engines*.

Corbin, J. C., Peng, W., Yang, J., Sommer, D. E., Trivanovic, U., Kirchen, P., Miller, J. W., Rogak, S., Cocker, D. R., Smallwood, G. J., Lobo, P., & Gagné, S. (2020). Characterization of particulate matter emitted by a marine engine operated with liquefied natural gas and diesel fuels. *Atmospheric Environment*, *220*. https://doi.org/10.1016/j.atmosenv.2019.117030

Dieselnet. (2022). https://dieselnet.com/standards/cycles/iso8178.php

European Commission. (2022). *Methane emissions*. https://energy.ec.europa.eu/topics/oil-gas-and-coal/methane-emissions_en

Proposal for a Regulation of the European Parliament and of the Council on type-approval of motor vehicles and engines and of systems, components and separate technical units intended for such vehicles, with respect to their emissions and battery durability (Euro 7) and repealing Regulations (EC) No 715/2007 and (EC) No 595/2009, (2022). https://ec.europa.eu/commission/presscorner/detail/en/ip_22_6495

European Commission. (2023). *Liquefied natural gas*. https://energy.ec.europa.eu/topics/oil-gas-and-coal/liquefied-natural-gas_en

European Parliament. (2022a). *Amendments adopted for proposal to amend Directive 2003/87/EC*.

European Parliament. (2022b). *Report on the proposal for a regulation of the European Parliament and of the Council on the use of renewable and low-carbon fuels in maritime transport and amending Directive 2009/16/EC*.

Global Methane Pledge, (2021). https://www.globalmethanepledge.org/

Grönholm, T., Makela, T., Hatakka, J., Jalkanen, J. P., Kuula, J., Laurila, T., Laakso, L., & Kukkonen, J. (2021). Evaluation of Methane Emissions Originating from LNG Ships Based on the Measurements at a Remote Marine Station. *Environmental Science and Technology*, *55*(20), 13677–13686. https://doi.org/10.1021/acs.est.1c03293

Heywood, J. (2019). *Internal Combustion Engine Fundamentals 2nd Edition*. McGraw Hill.

IMO. (2022a). *Data collection system for fuel oil consumption of ships*. https://www.imo.org/en/OurWork/Environment/Pages/Data-Collection-System.aspx

IMO. (2022b). *International Code of Safety for Ship Using Gases or Other Low-flashpoint Fuels (IGF Code)*. https://www.imo.org/en/OurWork/Safety/Pages/IGF-Code.aspx

IMO. (2022c). *Nitrogen Oxides (NOx) - Regulation 13*. https://www.imo.org/en/OurWork/Environment/Pages/Nitrogen-oxides-(NOx)-%E2%80%93-Regulation-13.aspx

International Gas Union. (2022). *2022 WORLD LNG REPORT*. https://www.igu.org/resources/world-lng-report-2022/

Johansson, L., Jalkanen, J. P., & Kukkonen, J. (2017). Global assessment of shipping emissions in 2015 on a high spatial and temporal resolution. *Atmospheric Environment*, *167*, 403–415. https://doi.org/10.1016/j.atmosenv.2017.08.042

Krivopolianskii, V., Valberg, I., Stenersen, D., Ushakov, S., & Æsøy, V. (2019). Control of the combustion process and emission formation in marine gas engines. In *Journal of Marine Science and Technology (Japan)* (Vol. 24, Issue 2, pp. 593–611). Springer Tokyo. https://doi.org/10.1007/s00773-018-0556-0

Kuczynski, S., Łaciak, M., Szurlej, A., & Włodek, T. (2020). Impact of liquefied natural gas composition changes on methane number as a fuel quality requirement. *Energies*, *13*(19). https://doi.org/10.3390/en13195060

Lehtoranta, K., Aakko-Saksa, P., Murtonen, T., Vesala, H., Ntziachristos, L., Rönkkö, T., Karjalainen, P., Kuittinen, N., & Timonen, H. (2019). Particulate Mass and Nonvolatile Particle Number Emissions from Marine Engines Using Low-Sulfur Fuels, Natural Gas, or Scrubbers. *Environmental Science and Technology*, *53*(6), 3315–3322. https://doi.org/10.1021/acs.est.8b05555

Lehtoranta, K., Murtonen, T., Vesala, H., Koponen, P., Karjalainen, P., Ntziachristos, L., Kuittinen, N., Alanen, J., Rönkkö, T., Keskinen, J., Aurela, M., & Timonen, H. (2017). Particle and gaseous emissions from a dual-fuel marine engine. *Paper Presented at 22nd International Transport and Air Pollution Conference, TAP 2017, Zürich, Switzerland.*

Lindstad, E., Eskeland, G. S., Rialland, A., & Valland, A. (2020). Decarbonizing maritime transport: The importance of engine technology and regulations for LNG to serve as a transition fuel. *Sustainability (Switzerland)*, *12*(21), 1–19. https://doi.org/10.3390/su12218793

Mærsk Mc-Kinney Møller Center for Zero Carbon Shipping. (2022). *An overview of methane emission sources and levels onboard vessels and the technologies, solutions, and regulatory drivers that can help reduce them.*

Myhre, G., Shindell, D., Bréon, F., Collins, W., Fuglestvedt, J., Huang, J., Koch, D., Lamarque, J., Lee, D., Mendoza, B., Nakajima, T., Robock, A., Stephens, G., Takemura, T., Zhang, H., Qin, D., Plattner, G., Tignor, M., Allen, S., … Midgley, P. (2013). *Anthropogenic and Natural Radiative Forcing. In: Climate Change 2013: The Physical Science Basis. Contribution of Working Group I*.

Pavlenko, N., Comer, B., Zhou, Y., Clark, N., & Rutherford, D. (2020). *The climate implications of using LNG as a marine fuel*. www.theicct.org

Peng, W., Yang, J., Corbin, J., Trivanovic, U., Lobo, P., Kirchen, P., Rogak, S., Gagné, S., Miller, J. W., & Cocker, D. (2020). Comprehensive analysis of the air quality impacts of switching a marine vessel from diesel fuel to natural gas. *Environmental Pollution*, *266*. https://doi.org/10.1016/j.envpol.2020.115404

Plevrakis, G., Koutsourakis, P., Stamopoulos, S., Sarvaiya, J., Soultanias, I., Vaidhyanathan, S., Seward, N., Shen, T., Zhu, A., Koliniati, R., Kalamidas, A., Barcarolo, D., Dimakopoulos, I., Zhang, A.-N., Daiyan, H., Bose, A., Bell, S., Bass, L., Crisafulli, S., & Lashbrook, J. (2022). *Setting the course to low carbon shipping*.

Rolls-Royce. (2012). *Rolls-Royce Marine-The "Environship Concept" System Solutions & Wave Piercing Technology*.

Schuller, O., Kupferschmid, S., Hengstler, J., & Whitehouse, S. (2021). *Title: 2 nd Life Cycle GHG Emission Study on the Use of LNG as Marine Fuel*.

Sommer, D. E., Yeremi, M., Son, J., Corbin, J. C., Gagné, S., Lobo, P., Miller, J. W., & Kirchen, P. (2019). Characterization and Reduction of In-Use CH 4 Emissions from a Dual Fuel Marine Engine Using Wavelength Modulation Spectroscopy. *Environmental Science and Technology*, *53*(5), 2892–2899. https://doi.org/10.1021/acs.est.8b04244

Stenersen, D., & Thonstad, O. (2017). *SINTEF Ocean AS Maritim GHG and NOx emissions from gas fuelled engines*. www.sintef.no/ocean

Ushakov, S., Stenersen, D., & Einang, P. M. (2019). Methane slip from gas fuelled ships: a comprehensive summary based on measurement data. In *Journal of Marine Science and Technology (Japan)* (Vol. 24, Issue 4, pp. 1308–1325). Springer. https://doi.org/10.1007/s00773-018-00622-z

Winterthur Gas & Diesel Ltd. (2019). *Greenhouse Gas (GHG) Emissions from LNG Engines, Review of the Two-Stroke Engine Emission Footprint 4-Emission Reduction Technologies-What's in Store for the Future*. https://www.cimac.com.

APPENDIX A. List of engines with the identifier names used in this study and respective references. Engines of same type in same year are marked with running alphabets. Engines for which measurements are conducted in testbed are marked with asterisk (*), for others, measurements were conducted on-board.

Engine identifier in this study	Engine type*	Stroke	Speed class	Rated speed	Engine year*	Max power (MW)	Reference
LPDF 4-S 2012, MGO	LPDF	4-S	medium speed	500	2012	7.6	Anderson et al. 2015
LPDF 4-S 2012	LPDF	4-S	medium speed	500	2012	7.6	Anderson et al. 2015
LBSI 4-S < 2010 (a)	LBSI	4-S			< 2010		Ushakov et al. 2019
LBSI 4-S > 2010 (a)	LBSI	4-S			> 2010		Ushakov et al. 2019
LBSI 4-S > 2010 (b)	LBSI	4-S			> 2010		Ushakov et al. 2019
LBSI 4-S 2015	LBSI	4-S	medium speed	900	2015	1.46	Ushakov et al. 2019
LBSI 4-S > 2010 (c)	LBSI	4-S			> 2010		Ushakov et al. 2019
LBSI 4-S> 2010 (d)*	LBSI	4-S			> 2010		Ushakov et al. 2019
LBSI 4-S > 2010 (e)*	LBSI	4-S			> 2010		Ushakov et al. 2019
LBSIs 4-S > 2010	LBSI	4-S			> 2010		Ushakov et al. 2019
LPDF > 2013 (a)	LPDF	na			> 2013		Ushakov et al. 2019
LPDF > 2013 (b)*	LPDF	na			> 2013		Ushakov et al. 2019
LPDF 4-S > 2013	LPDF	4-S		750	> 2013	3	Ushakov et al. 2019

LPDF > 2013 (c)*	LPDF	na			> 2013		Ushakov et al. 2019
LPDF > 2013 (d)*	LPDF	na			> 2013		Ushakov et al. 2019
LPDF > 2013 (e)*	LPDF	na			> 2013		Ushakov et al. 2019
LPDF > 2013 (f)*	LPDF	na			> 2013		Ushakov et al. 2019
LPDFs > 2013	LPDF	na			> 2013		Ushakov et al. 2019
LBSI 4-S 2016 (a)*	LBSI	4-S					Rolls Royce. according to Stenersen & Thonstadt 2016
LBSI 4-S 2016 (b)*	LBSI	4-S					Rolls Royce. according to Stenersen & Thonstadt 2016
LPDF 4-S 2016 (a)*	LPDF	4-S					Wartsila. according to Stenersen & Thonstadt 2016
LPDF 4-S 2016 (b)*	LPDF	4-S					Wartsila. according to Stenersen & Thonstadt 2016
LPDF 4-S 2016 (c)*	LPDF	4-S					Wartsila. according to Stenersen & Thonstadt 2016
LBSI 4-S 2016 (c)*	LBSI	4-S				0.5	Mitsubishi Turbocharger and Engine Europe B.V.. according to Stenersen & Thonstadt 2016
LPDF 4-S 2016 (d)	LPDF	4-S	medium-speed	720	2016	4.32	Corbin et al. 2020, Sommer et al. 2019, Peng et al. 2020
LPDF 4-S 2016 (d), ULSD	LPDF	4-S	medium-speed	720	2016	4.32	Corbin et al. 2020

LPDF 4-S 2016 (e)	LPDF	4-S	medium-speed	720	2016	4.32	Sommer et al. 2019
LPDF 2-S 2021 (a)	LPDF	2-S	low-speed	60	2021	11.53	Balcombe et al. 2022
LPDF 2-S 2021 (b)	LPDF	2-S	low-speed	60	2021	11.53	Balcombe et al. 2022
LPDF 4-S 2021 (c)	LPDF	4-S	medium-speed	720	2021	3.84	Balcombe et al. 2022
LPDF 4-S 2021 (d)	LPDF	4-S	medium-speed	720	2021	2.88	Balcombe et al. 2022
LPDF 4-S 2021 (e)	LPDF	4-S	medium-speed	720	2021	2.88	Balcombe et al. 2022
LPDF 4-S 2021 (f)	LPDF	4-S	medium-speed	720	2021	3.84	Balcombe et al. 2022
LPDF 4-S retrofitted 2016*	LPDF	4-S	medium speed	750	retrofitted 2016	1.4	Lehtoranta et al. 2019 and VTT database, Alanen et al. 2020
LBSI 4-S, publ. 2012*	LBSI	4-S					Rolls Royce 2012
LPDF 2-S, publ. 2018*	LPDF	2-S					WinGD, according to Pavlenko et al. 2020
HPDF 2-S, publ. 2020*	HPDF	2-S	slow speed				MAN, according to Lindstad 2020
HPDFs 2-S 2020*	HPDF	2-S	slow speed		2020		Different manufacturers, according to SPHERA 2021
LPDFs 2-S 2020*	LPDF	2-S	slow speed		2020		Different manufacturers, according to SPHERA 2021

GREEN RAY

LBSIs 4-S 2020*	LBSI	4-S	medium-speed	2020		Different manufacturers, according to SPHERA 2021
LPDFs 4-S 2020*	LPDF	4-S	medium-speed	2020		Different manufacturers, according to SPHERA 2021
HPDFs 2-S, publ. 2022*	HPDF	2-S				Data from engine manufacturers, according to Mærsk Mc-Kinney Møller Center for Zero Carbon Shipping
LPDFs wo EGR 2-S, publ. 2022*	LPDF wo EGR	2-S				Data from engine manufacturers, according to Mærsk Mc-Kinney Møller Center for Zero Carbon Shipping
LPDFs with EGR 2-S, publ. 2022*	LPDF with EGR	2-S				Data from engine manufacturers, according to Mærsk Mc-Kinney Møller Center for Zero Carbon Shipping
LPDFs with EGR 4-S, publ. 2022*	LPDF	4-S				Data from engine manufacturers, according to Mærsk Mc-Kinney Møller Center for Zero Carbon Shipping
LPDF 2-S 2020 (a)*	LPDF	2-S	low speed	2020	>50	Ship owner data
LPDF 2-S 2020 (b)*	LPDF	2-S	low speed	2020	>50	Ship owner data
LPDF 2-S 2021 (c)*	LPDF	2-S	low speed	2021	>50	Ship owner data
LPDF 2-S 2021 (d)*	LPDF	2-S	low speed	2021	>50	Ship owner data
LPDF 2-S 2021 (e)	LPDF	2-S	low speed	2021	>50	Ship owner data
LPDF 2-S 2019	LPDF	2-S	low speed	2019	<12	Ship owner data

LPDF 4-S 2019 (a)*	LPDF	4-S	medium speed	2019	<4	Ship owner data
LPDF 4-S 2020*	LPDF	4-S	medium speed	2020	<3	Ship owner data
LPDF 4-S 2022 (a)*	LPDF	4-S	medium speed	2022	<4	Ship owner data
LPDF 4-S 2019 (b)*	LPDF	4-S	medium speed	2019	<4	Ship owner data
LPDF 4-S 2022 (b)*	LPDF	4-S	medium speed	2022	<4	Ship owner data
LPDF 4-S 2017*	LPDF	4-S	medium speed	2017	1	Lehtoranta et al. 2019

APPENDIX B. Other gaseous emissions (carbon dioxide, carbon monoxide, total hydrocarbons, non-methane hydrocarbons, formaldehyde, and nitrous oxides) reported for the included engines. For NO_x lines are included to help interpreting the load behavior of different engines.

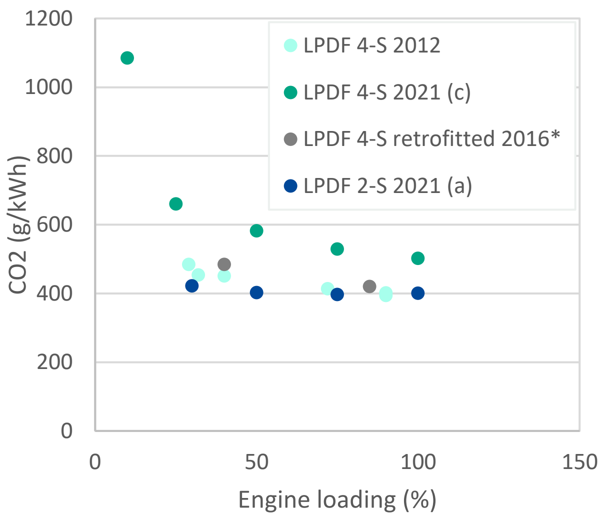

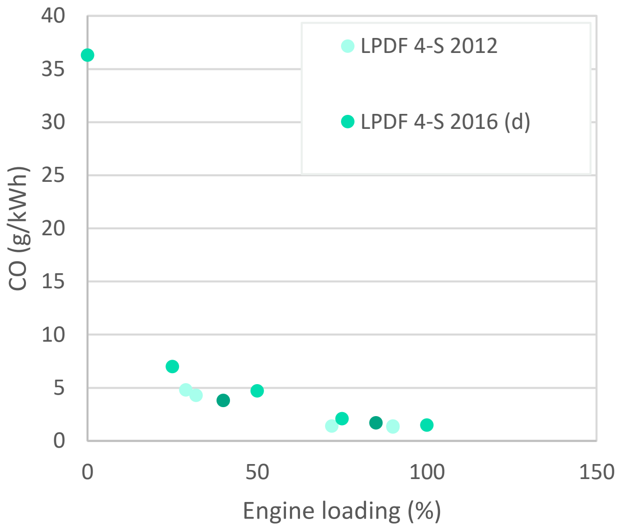

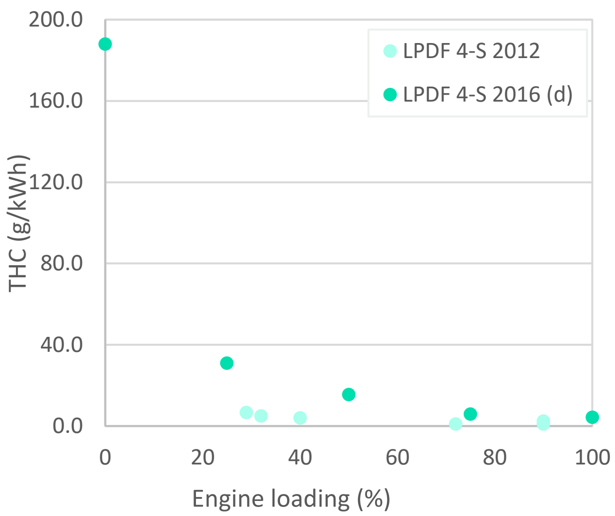

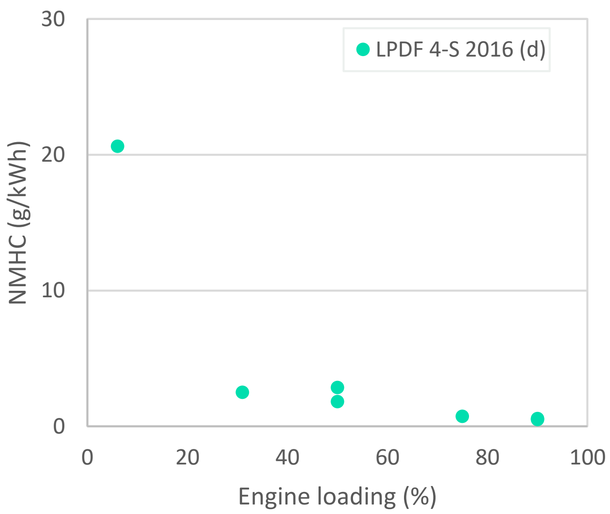

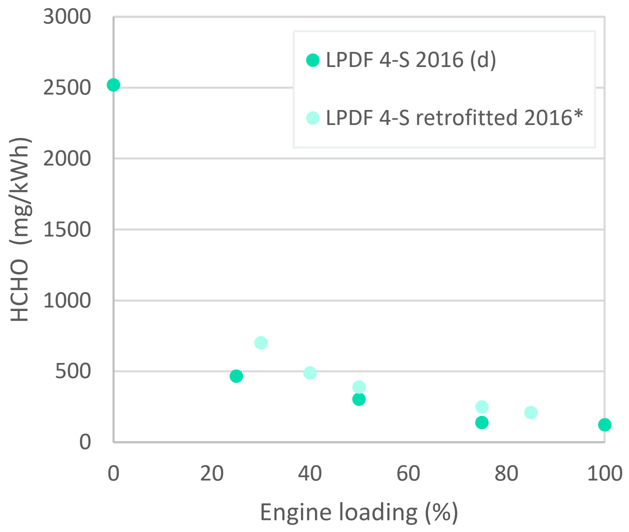

3000
2500
2000
1500
1000
500
0
HCHO (mg/kWh)
0
20
40
60
80
100
Engine loading (%)
LPDF 4-S 2016 (d)
LPDF 4-S retrofitted 2016*

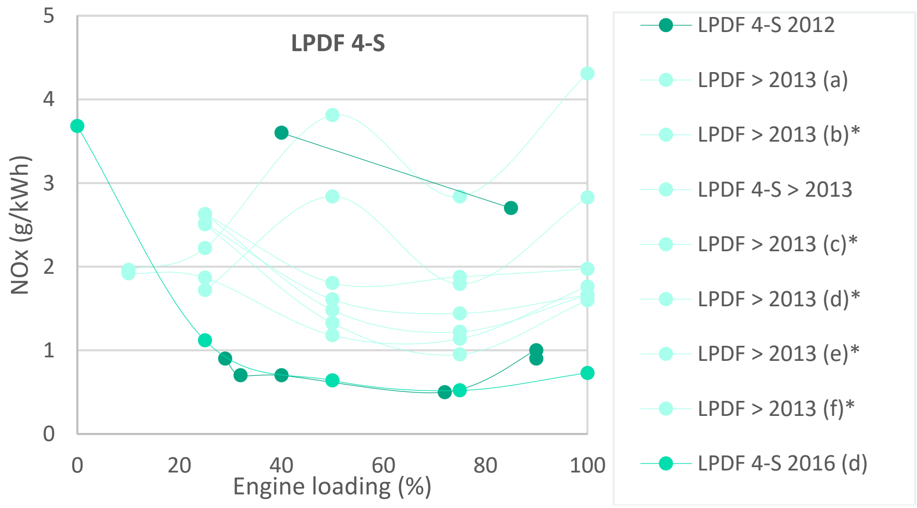

LPDF 4-S
5
4
3
2
1
0
NOx (g/kWh)
0
20
40
60
80
100
Engine loading (%)
LPDF 4-S 2012
LPDF > 2013 (a)
LPDF > 2013 (b)*
LPDF 4-S > 2013
LPDF > 2013 (c)*
LPDF > 2013 (d)*
LPDF > 2013 (e)*
LPDF > 2013 (f)*
LPDF 4-S 2016 (d)

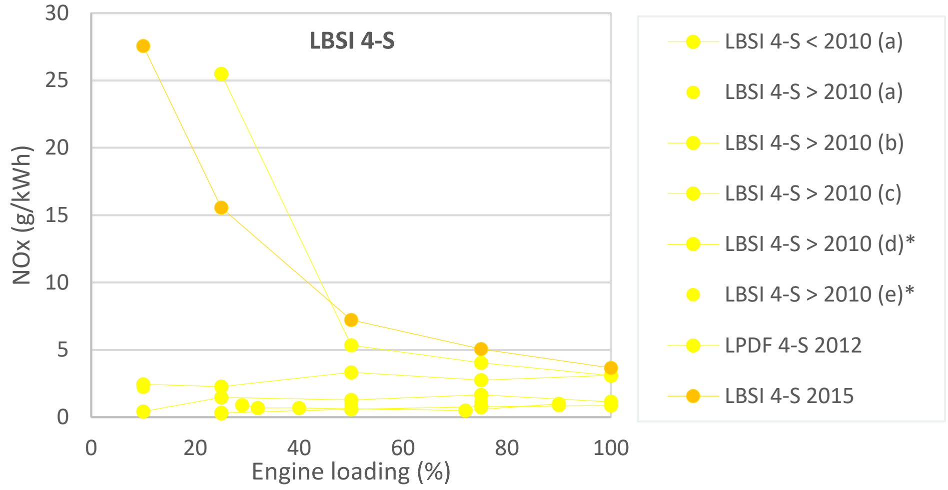
LBSI 4-S
NOx (g/kWh)
30
25
20
15
10
5
0
0
20
40
60
80
100
Engine loading (%)
LBSI 4-S < 2010 (a)
LBSI 4-S > 2010 (a)
LBSI 4-S > 2010 (b)
LBSI 4-S > 2010 (c)
LBSI 4-S > 2010 (d)*
LBSI 4-S > 2010 (e)*
LPDF 4-S 2012
LBSI 4-S 2015

APPENDIX C. Particulate emissions (total particle mass, non-volatile particle mass, total particle number, non-volatile particle number, elemental and organic carbon, black carbon) reported for the included LNG engines.

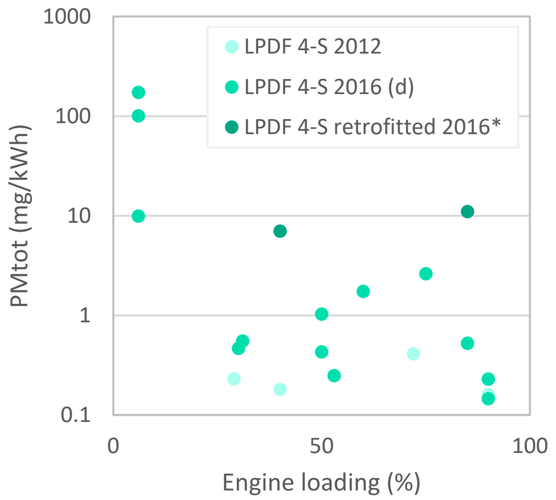

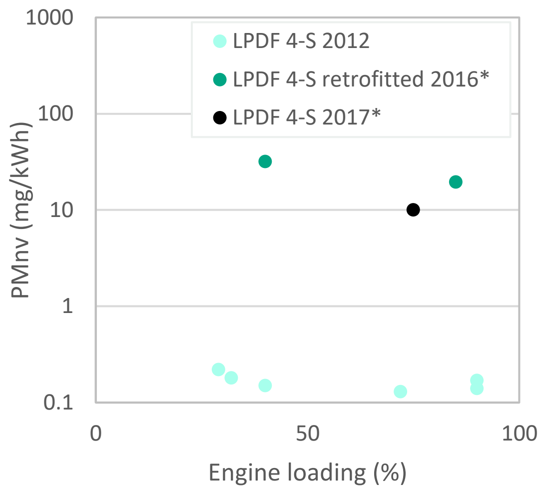

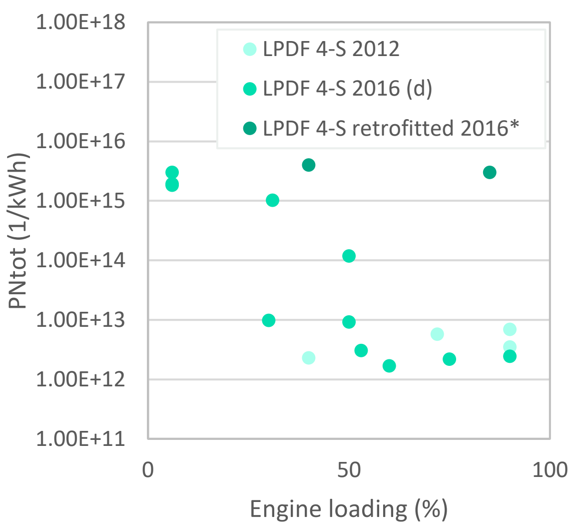

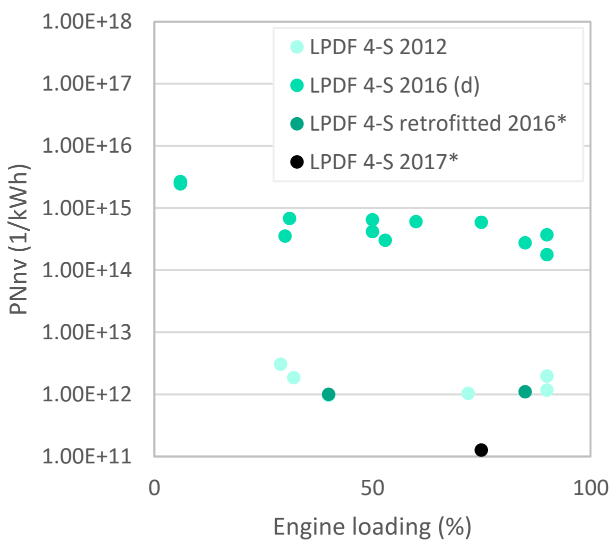

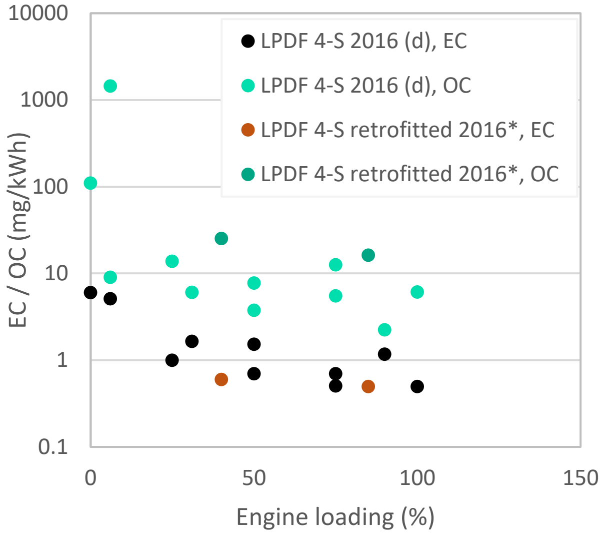

10000
1000
100
10
1
0.1
EC / OC (mg/kWh)
LPDF 4-S 2016 (d), EC
LPDF 4-S 2016 (d), OC
LPDF 4-S retrofitted 2016*, EC
LPDF 4-S retrofitted 2016*, OC
0
50
100
150
Engine loading (%)

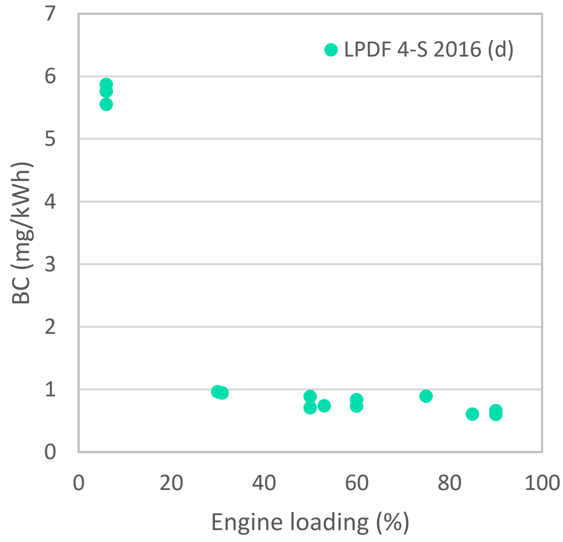

7
6
5
4
3
2
1
0
BC (mg/kWh)
LPDF 4-S 2016 (d)
0
20
40
60
80
100
Engine loading (%)